REVIEW

Check for updates

Polymer-based nanocomposites for heavy metal ions removal from aqueous solution: a review

Guixia Zhao, [ID] [a] Xiubing Huang, [ID] [b] Zhenwu Tang, [ID] [a] Qifei Huang,[c] Fenglei Niu[a] and Xiangke Wang [ID] *[a]

Water pollutant treatment has become a critical issue in environmental engineering and protection. Adsorption techniques *via* solid adsorbents have been widely applied for the efficient removal of metal ions from wastewater solutions, where polymer-based composites have attracted much attention due to their intrinsic environmentally harmless and degradable properties. Particularly, polymer-based nano-composites often present superior physical, chemical and mechanical properties, as well as superior compatibility, as compared with single polymers, by incorporating the advantages of both counterparts in the composites. This article is an overview of the versatile polymer-based composites containing different functional organic and/or inorganic counterparts for the removal of hazardous metal ions from waste-water. The synthesis of the adsorbents, adsorption process features and mechanism investigation are highlighted and discussed in detail. The future perspectives and trends in this field are also outlined. We hope that this review will provide some inspiring information for designing and fabricating polymer-based nanocomposites for the removal of diverse heavy metal ions from aqueous solution, and pollution management in the near future.

1. Introduction

With rapid urbanization and industrialization, hazardous metal pollution is among the most serious environmental issues that endanger human beings all over the world.[1,2] Although there have been several techniques for the removal of heavy metal ions, such as ion-exchange, reserve osmosis, chemical precipitation and electrochemical treatment, *etc.*, it is still challenging to achieve efficient and economical treatment approaches.[3] The adsorption technique is one of the most efficient and facile approaches to remove heavy metal ions such as Ni(II),[4] Co(II),[5] Cd(II),[5] Cu(II),[6] Cr(VI),[7] Pb(II)[8-10] from aqueous systems. To date, different kinds of nano-materials have been applied as adsorbents, including activated carbons (ACs),[11] clays,[12] metal oxides like Al_2O_3,[13,14] TiO_2,[15,16] SiO_2,[17] graphene materials,[5] polymers[18-20] and so on.[21-25] For example, Deliyanni *et al.* reviewed the application of activated carbon as an adsorbent for heavy metal removal, especially on Pb(II) and As(V).[26] The authors indicated the highest adsorp-

tion capabilities of 389 mg g^{-1} over oxidized carbon for Pb(II) and 33 mg g^{-1} over activated carbon inorganic composites for arsenic removal.[26] Also, in the review by Hua *et al.*, pure nano-sized metal oxides presented relatively low adsorption abilities for heavy metals from aqueous systems, although their specific surface area is high.[27] Generally, these inorganic adsorbents often suffer from the shortage of surface chelating groups and the resulting poor adsorption performances. Even for graphene materials with large surface areas, the performance of raw graphene adsorbents is still not satisfactory,[28,29] while for polymer adsorbents, the perfect skeleton strength, adjustable surface functional groups, feasible regeneration, environmental harmlessness and degradable properties are indeed suitable for application as potential adsorbents.[30-34] It was found that various organic and inorganic pollutants can be efficiently removed by polymers.[35] However, for practical applications, the low adsorption capacity and selectivity still need improvement, as well as the high degree of swelling and poor mechanical stability.

In recent years, in order to further improve the adsorption performance of polymeric materials, surface functionalization of polymers to obtain polymer-based composites has been considered an effective strategy on the basis that the incorporated functional counterparts would provide more specific inter-action with the target pollutants or improve the available surface adsorption properties of the polymer host.[31] Thus, polymer/polymer hybrids and polymer/inorganic hybrids have

*[a]School of Environment and Chemical Engineering, North China Electric Power University, Beijing, 102206, China. E-mail: xkwang@ncepu.edu.cn;
Fax: +86-10-61772890; Tel: +86-10-61772890*
[b]School of Materials Science and Engineering, University of Science and Technology Beijing, Beijing, 100083, China
[c]State Key Laboratory of Environmental Criteria and Risk Assessment, Chinese Research Academy of Environmental Sciences, Beijing 100012, China

emerged either by incorporating two different polymers or by irreversibly dispersing inorganic nanoparticles within polymer supports. Through the combination of two counterparts at the nanoscale, the resulting composites not only retain the inherent properties but also often show higher processability, greater stability, and even interesting improvements caused by the interactions of the nanoparticle-matrix. In the case of polymer/polymer composites, the disadvantages like low adsorption capacity, disintegration in aqueous solution or aggregation in alkaline solution can be significantly improved in the polymer hybrids.[36,37] In the case of polymer/inorganic nanoparticle composites, the incorporated nanoparticles are easy to separate from the adsorption system without the potential release into the environment, but they still maintain unique inherent physical and chemical properties.[38,39] The polymer matrix has proved to be an ideal support for the fabrication of composites as adsorbents, considering the adjustable surface functionality and the excellent mechanical strength.[40] The nanoparticles encapsulated in the composites are separated within the polymer matrix and are less aggregated with each other. Moreover, the functional groups from the immobilized counterparts are beneficial for the permeation of inorganic pollutants.[40,41]

In the present review, recent techniques and advances in the synthesis of polymer-based composites and applications on pollutant treatment in aqueous systems are summarized and discussed. The synthesis methods are overviewed in detail, and the applications in pollutant removal are classified according to the composite types such as copolymer composites, polymer/carbon material composites, polymer/clay mineral composites, magnetic polymer composites and polymer/metal composites.

2. Preparation of polymer-based composites

There are different classifications for the preparation methods. One classification is based on the formation process of the counterparts, by which the preparation methods can be generally divided into two categories called *in situ* synthesis and direct compounding.[31] Another classification is more meticulous, according to the detailed preparation paths, by which the synthesis methods include (i) self-assembly processes; (ii) sol–gel processes; (iii) dispersion or assembling of nano-building blocks; (iv) interpenetrating networks and hierarchical structures.[42] Herein, a new classification is introduced according to the formation sequence of both counterparts, in which the preparations can be divided into three categories: (i) support-host method, (ii) assemble building-block method and (iii) interpenetrating method.

2.1. Support-host method

In this method, one of the counterparts in the composites is synthesized first and used as a support to host the other counterpart as the guest. This method is convenient in operation, suitable for massive production and is comparatively cost-efficient; it includes the following two types: (i) the polymer matrix serves as the support, where the precursors for the other counterpart are preloaded within the polymer matrix for the post-synthesis of the target counterpart. (ii) The other counterpart serves as the pre-formed support, and the monomers of the polymer serve as the guests for post-polymerization, where the monomers are first mixed with the counterpart and then polymerized under desirable conditions. The former strategy has been widely used to prepare polymer com-

Guixia Zhao received her B.S. degree from Lanzhou University in 2009 and her Ph.D. degree from the Institute of Plasma Physics, Chinese Academy of Sciences under the supervision of Prof. Xiangke Wang in 2014. While working on her Ph.D., Guixia joined Prof. John T. S. Irvine's research group at the University of St Andrews as a visiting student for one year, working on water splitting photocatalysis under visible light.

Guixia Zhao

After visiting for several months in Prof. John T. S. Irvine's research group and two years as a JSPS postdoctoral fellow at National Institute for Materials Science (NIMS) under the supervision of Prof. Jinhua Ye, Dr Zhao now is a Humboldt Research Fellow at Ruhr-University Bochum under the supervision of Prof. Martin Muhler. Dr Zhao has broad research interests in wastewater treatment, photocatalysis and materials chemistry.

Xiubing Huang received his B.E. and M.S. degree from the University of Science and Technology Beijing (China), and a Ph.D. degree (advisor: Prof. John T. S. Irvine) from the School of Chemistry at the University of St Andrews (UK) in 2015. After one year of post-doctoral work at the Research Centre for Materials Science of Nagoya University (Japan), he was appointed as a lecturer in the School of Materials Science

Xiubing Huang

and Engineering at the University of Science and Technology Beijing. Currently, Dr Huang has broad interests in nanostructured materials in environment and energy-related applications.

posites like polymer/polymer hybrids,[37] polyaniline (PANI)/ metallic iron nanocomposites,[43] amorphous calcium carbonate nanoparticles stabilized by polyacrylic acid,[44] hydrolyzed polyacrylamide (PAM) modified xanthan gum/nanosilica composites,[45] and polystyrene (PS)-supported zirconium phosphate nanoparticles.[46] For instance, poly(methyl methacrylate) (PMMA) cored amphiphilic nanoparticles with polyethyleneimine (PEI) shelled amphiphilic nanoparticles were synthesized successfully by a one-step emulsifier-free polymerization method using PEI as the preformed host (Fig. 1a).[37] Bhaumik et al.[43] presented a simple preparation for PANI/ metallic iron nanocomposites at room temperature. First PANI was synthesized through the polymerization of aniline monomers with Fe(III) chloride as the oxidant. The by-products from the polymerization were then used as Fe precursor for the reductive deposition of Fe nanoparticles.[43] To ensure that the precursors were dispersed into the inner pores of the polymeric support, the suspension containing polystyrene support and $ZrOCl_2$ was evaporated and then added to H_3PO_4 and agitated.[46] In this case, it is worth noting that the harsh post-loading conditions may lead to polymer degradation.

The latter strategy has been successfully used to prepare ferromagnetic amine polymer composites,[38] PANI/multiwalled carbon nanotube (PANI/MWCNTs) magnetic composites,[39] polyacrylonitrile/organobentonite composites[47] and PANI/ α-zirconium phosphate.[48] For example, amidoxime functionalized polyacrylonitrile/organobentonite composites were prepared by the in situ intercalation polymerization technique.[47] Attention should be paid to the good dispersion of the counterpart within the liquid monomers to avoid the single-phase aggregation. In our group, MWCNTs were grafted with PANI molecules by a plasma-induced grafting technique to form PANI/MWCNTs composites.[39] In some cases, core–shell
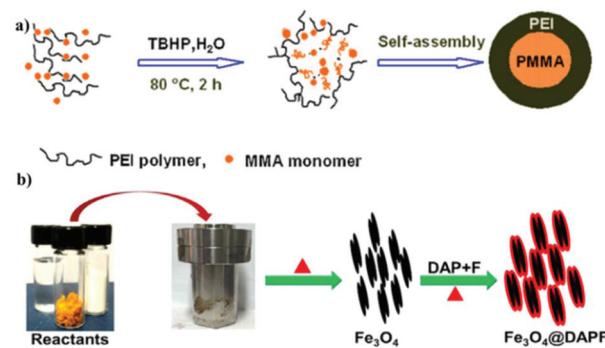
Fig. 1 (a) Synthesis of PMMA/PEI core–shell nanoparticles. Reproduced with permission from ref. 37. Copyright 2011 Elsevier. (b) Schematic Illustration of the Synthesis of Fe_3O_4@DAPF ferromagnetic nanorods. Reproduced with permission from ref. 38. Copyright 2015 American Chemical Society.

structures can be formed.[49,50] Venkateswarlu and Yoon used 2,3-diaminophenol and formaldehyde (DAPF)-based polymer to modify the surface of twin-like Fe_3O_4 ferromagnetic nanorods and prepared Fe_3O_4@DAPF ferromagnetic nanorods (Fig. 1b).[38] Wang et al. synthesized Fe_2O_3@polystyrene core–shell nanoparticles using solvent-free atom transfer radical polymerization (ATRP), in which Fe_2O_3 nanoparticles were stabilized using oleic acid and exchanged with the initiator for ATRP, 2-bromo-2-methylpropionic acid (Br-MPA). These Fe_2O_3 nanoparticles were soluble in styrene and were used as macro-initiators for the solvent-free ATRP. In this way, polymerization was restricted to the nanoparticle surfaces in the ATRP reaction, the uniform shell layers became obtainable, and thus well-defined Fe_2O_3@PS nanoparticles were prepared.[49] Recently, by the facile interfacial polymerization of trimesoyl

Zhenwu Tang is a professor at the North China Electric Power University. He received his M.E. degree in 2004 from Southwest University, China, and his Ph.D. in 2007 from Beijing Normal University. His focus is on the environmental behaviors and ecological risks of emerging pollutants, and also environmental risk and its control during the recycling of solid waste. He has published over 60 papers in peer-reviewed journals.

Zhenwu Tang

Prof. Qifei Huang is an environmentalist working at the State Key Laboratory of Environmental Criteria and Risk Assessment, Chinese Research Academy of Environmental Sciences. He graduated from Southwest University, China, in 1996, and received his Ph.D. in 2002 from Institute of Geographic Sciences and Natural Resources Research, Chinese Academy of Sciences. He is closely engaged in the pollution control of solid waste and

Qifei Huang

hazardous chemicals. He has authored or co-authored over 250 papers in peer-reviewed journals and 8 books. As chief editor, he has edited 2 international and 13 national environmental standards/guidelines. He got 15 authorized national patents and was awarded 8 provincial-level scientific and technological progress awards of China.

chloride 0.1% (w/v) in *n*-hexane solution and a solution of *m*-phenylenediamine 2% (w/v) in water, the graphene oxide (GO) nanosheets were dispersed and graphene was modified with polyamide to synthesize an effective composite. The resulting composites offered great promise for the efficient elimination and remediation of Sb(III) ions from solution, due to their fast and high sorption capacities.[51]

2.2. Assemble building-block method

In this method, the two counterparts in the composites are pre-formed separately and then assembled together through good interactions such as van der Waals forces, weak hydrogen bonding, or electric/magnetic dipole. Usually, the desirable size of the resulting composites can be controlled by this approach;[52,53] nevertheless, it is difficult to decide the space distribution parameters of the guest in or on the support matrix and the guest usually aggregates during blending. By adding appropriate dispersant or compatibilizers, the guest particle dispersion and the interaction between guest and support host can be improved. For example, Yu *et al.*[54] synthesized the cellulose/TiO_2 composites in the presence of supercritical CO_2. The supercritical CO_2 influenced the interactions among the molecular cellulose chains and through the formation of hydrogen bonds with hydroxyl groups of cellulose, the titania particles were used to impregnate and access the crystalline structures of cellulose fibers, resulting in a great improvement of thermal stability. Naushad *et al.* prepared starch/SnO_2 nanocomposites through mixing the gel of SnO_2 and the dispersed solution of cross-linked starch under stirring and heating at 60 °C for 6 h, followed by treating with an excess of 1.0 M HNO_3, replacing the supernatant solution with fresh acid to complete the conversion of starch/SnO_2 compo-
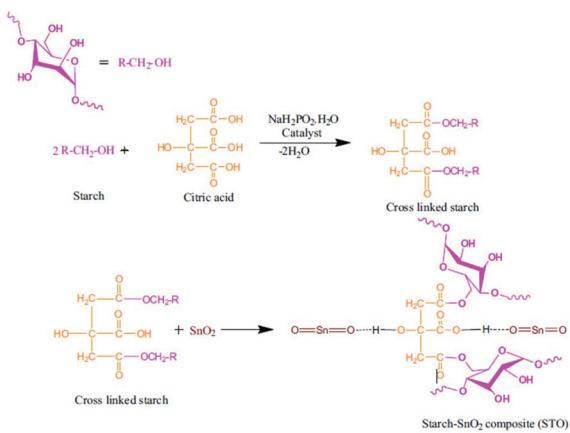

Fig. 2 Synthesis of starch/SnO_2 nanocomposites. Reproduced with permission from ref. 55. Copyright 2016 Elsevier.

sites into the H^+ form. SnO_2 and starch were mixed well *via* the intermolecular hydrogen bonding (Fig. 2).[55] Polymer nanocomposites constituted of [ethylene-vinyl acetate (EVA) (70%) polycaprolactone (PCL) (15%) Fe_3O_4 (15%)] were also prepared simply by assembly mixing EVA, PCL and Fe_3O_4 in the molten state in an extruder equipped with roller rotors.[56] This simple assembling method was successful in the preparation of magnetic composites composed of superparamagnetic Fe_2O_3 nanoparticles and β-cyclodextrin with a core–shell nanostructure.[57]

2.3. Interpenetrating method

In this method, the two counterparts in the composites are formed at the same time by homogeneously blending the precursors of the polymers and the other counterparts, by which

Fenglei Niu is a professor of North China Electric Power University. He received his Ph.D. in 2003 from University of California, Berkeley, and then he worked as a postdoc research associate at Los Alamos National Laboratory (2005–2007) and a technologist at GE Company (2007–2010). His research focuses on environmental pollution from nuclear fuels and nuclear materials. He has published over 100 journal articles, conference publications, and technical reports on these topics.

Fenglei Niu

Xiangke Wang is a professor of North China Electric Power University. He received his Ph.D. in 2000 from Lanzhou University. Then he joined the SUBATECH Laboratory (France) as a research fellow and the Karlsruhe Research Center (Germany) as an Alexander von Humboldt research fellow. His focus is on the synthesis of nanomaterials and their applications in energy and environmental pollution management, and also characterization for radionuclide physicochemical behavior in the environment. He has published over 350 papers in peer-review journals with >22 000 citations, and his H-index is currently 88. He is also a highly cited researcher in the Environmental and Engineering areas by Thomson Reuters from 2014 to 2016, and by Clarivate Analytics in 2017.

Xiangke Wang

the resulting polymer composites are interpenetrated with each other even at the molecular scale. Regarding the interactions between the two counterparts in the resulting polymer composites, there are two types: (i) covalent bonds between the hybrids and (ii) weak interaction between the moieties.[58,59] A typical example for the first case is the successful commercial organic–inorganic hybrid polymers, *i.e.*, phenylsilsesquioxane–alkylsilsesquioxane copolymers, by Brady *et al.* in the 1950s. With precursors such as metal halides and metal alkoxides in water and organic solvents, a series of hydrolysis and condensation reactions *via* nucleophilic substitution mechanism led to the sol formation, where individual particles weakly interacted with each other and were converted into an integrated network due to cross-linking reactions (Fig. 3).[60] A gel was obtained after further drying processes. By modifying the structure of silsesquioxanes with different organic groups (R) such as R′(OR)$_2$Si–R–Si(OR)$_3$ precursor compounds, the resulting organic–inorganic network can be further modified.[61] In the second case, the two counterparts were only simultaneously formed into homogeneous composites without phase separation, but with no covalent interactions with each other. For instance, through undergoing radical free polymerization of 2-hydroxyethyl methacrylate (HEMA) with the simultaneous acid-catalyzed sol–gel reaction of the tetraethoxysilane (TEOS) precursor, optically transparent and homogeneous hybrid materials were formed.[62] Similarly, polyimide–silica gel hybrids were prepared *via* the simultaneous *in situ* formation of a silica network and polyimides through the hydrolysis and condensation of tetramethoxy-silane (TMOS) in *N,N*-dimethylacetamide (DMAc) solution containing 5% LiCl, ZnCl$_2$, or CaCl$_2$ and a polyimide intermediate.[63] Films were cast from the resulting mixtures and then the solvent was evaporated gradually, resulting in the formation of transparent, clear, amber-colored or pale yellow hybrid films, and the salts were well dispersed at the molecular level.[63]

There are three competing process in such a dual reaction: (i) formation of the inorganic phase by hydrolysis and condensation; (ii) polymerization of the organic phase; (iii) the thermodynamics of phase separation of the two phases. To avoid the phase separation, the dual reaction should occur simultaneously and rapidly enough.[58]

3. Removal of metal ions from wastewater solutions by polymer-based composites

Based on the different counterparts in the polymer-based composites, heavy metal ion removal by polymer-based composites will be overviewed according to the classifications of different kinds of composites, with a discussion of the structure and mechanism of the adsorbents and adsorption process.

3.1. Removal of heavy metals over copolymer composites

Compared with single polymer adsorbents, dual polymer composites exhibit more abundant surface groups, higher adsorp-
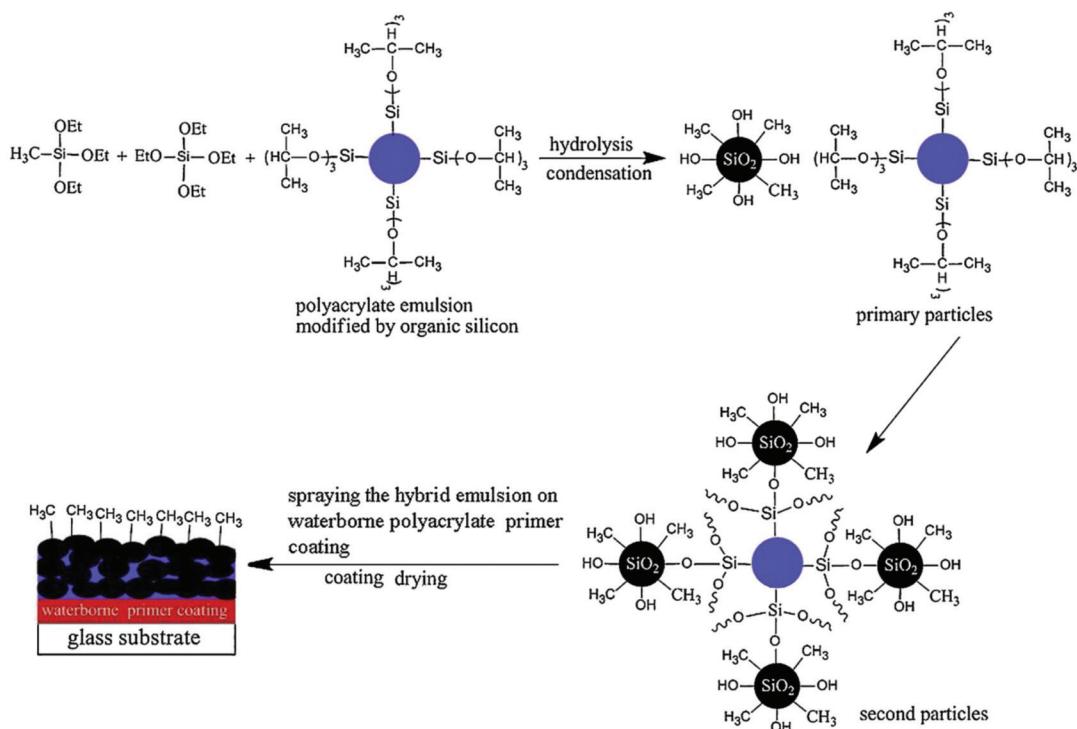

Fig. 3 Schematic illustration of sol–gel derived organic–inorganic hybrid coatings. Reproduced with permission from ref. 60. Copyright 2011 Elsevier.

tion capacity, better stability and mechanic feasibility.[64] Polypyrrole (PPy) has proved to be a suitable polymer to combine with other polymer counterparts like PANI,[65,66] polyacrylonitrile.[67] In detail, Co(II) adsorption on PANI/PPy polymer nanofibers with initial concentrations of 100 mg L^{−1} reached the removal efficiency of 99.68% in 11 min, and the sorption kinetics followed the pseudo-second-order model. Sorption isotherms fitted well to the Freundlich model and the maximum desorption efficiency was 90%, with good reuse performance after desorption processes.[65] Similarly, PPy-PANI nanofibers, prepared by the coupling of propagating PPy[•+] and PANI[•+] free radicals without a template through the simultaneous polymerization of aniline and pyrrole monomers in the presence of the FeCl$_3$ oxidant, were applied for Cr(VI) removal from wastewater. It was found that the adsorption of Cr(VI) was highly pH-dependent and the adsorption kinetics followed the pseudo-second-order model. The sorption isotherm data fitted well to the Langmuir model, and the maximum sorption capacity of PPy-PANI nanofibers for Cr(VI) was 227 mg g^{−1} with good selectivity and reusability after two adsorption–desorption cycles of operation. The adsorption processes were endothermic and spontaneous, and were marked with increases in randomness. A physicochemical process including ion-exchange followed by Cr(VI) reduction to Cr(III) using electron rich polymer nanofibers was the main uptake mechanism (Fig. 4).[68] Recently, Checkol et al. presented a highly stable and efficient hybrid material consisting of poly(3,4-ethylenedioxythiophene)/polystyrene sulfonate (PEDOT/PSS) and the biopolymer lignin (LG) for the elimination of metals. Results confirmed that Pb^{2+} was adsorbed on the composite films from a neutral solution when a negative potential was applied and was subsequently desorbed by applying a positive potential, with the sorption ability of 245.5 mg g^{−1}, which was almost doubled to 452.8 mg g^{−1} by incorporating LG into PEDOT/PSS.[69]

Another nanofiber composed of PPy/polyacrylonitrile core–shell structures was prepared for Cr(VI) removal from aqueous solutions.[67] The results indicated that Cr(VI) removal increased with the decrease in the initial solution pH. The equilibrium was reached in 30 to 90 min when the initial Cr(VI) concentration increased from 100 mg L^{−1} to 200 mg L^{−1}, and the kinetic process was well described by the pseudo-second-order model and the thermodynamic process was endothermic and spontaneous. The adsorption capacity remained at up to 80% after 5 cycles of desorption and usage. Cr(VI) reduction and ion exchange were the main mechanisms for Cr(VI) interaction according to the XPS analysis.[67]

Other copolymer composites such as amphiphilic nanoparticles with PMMA cores and PEI shells were applied as novel polymeric adsorbents to remove Cu(II) ions, with maximum sorption capacity of 14 mg g^{−1} obtained under simple and fast experimental conditions.[37] According to Yan et al.,[70] the magnetic composite microspheres (MCM), consisting of Fe$_3$O$_4$ nanoparticles and poly(acrylic acid) (PAA) blended chitosan (CS) were employed as adsorbents for Cu(II) removal from wastewater solutions. It was revealed that CS/PAA-MCM had higher sorption capacity than CS-MCM, which was mainly attributed to the interaction of Cu(II) with PAA in the composites. The adsorption kinetics followed the pseudo-second-order model and the adsorption isotherms were well fitted to the Langmuir model. Furthermore, the composites were well regenerated at low pH, without any loss of sorption capacity when reused. On the contrary, at pH greater than 4.0, the adsorbed Cu(II) ions were stable enough, and Cu-loaded adsorbents showed high phosphate removal efficiency at pH ranging from 4.0 to 8.0 in the secondary adsorption.[70]

3.2. Removal of heavy metals over polymer/carbon material composites

Carbonaceous materials such as CNTs, AC[71] and graphene are considered as promising counterparts in polymer-based composites due to the high mechanic strength, high aspect ratio and especially the compatibility of the carbon matrix with the polymeric structure for high dispersion carbon counterparts into the polymers and the sustenance of strong interaction and adhesion.[72] Typically, to simultaneously improve the permeability and filtration efficiency of polymer membranes, polyethylene glycol (PEG) and AC were added to polyetherimide (PEI)/polyphenylsulfone (PPSU) polymers to synthesize novel polymer membranes. It was found that the addition of AC significantly affected the pore size distribution, membrane morphology, chemical properties and porosity. The addition of PEG increased the surface porosity and hydrophilicity of the AC/PPSU/PEI/PEG membranes due to the formation of the hydrophilic pore. The intrinsic membrane resistances decreased with the increase in PEG concentration. The humic acid (HA) removal efficiency and optimum membrane permeability were 80% and 184 L (m^2 h)$^{-1}$, respectively, with the
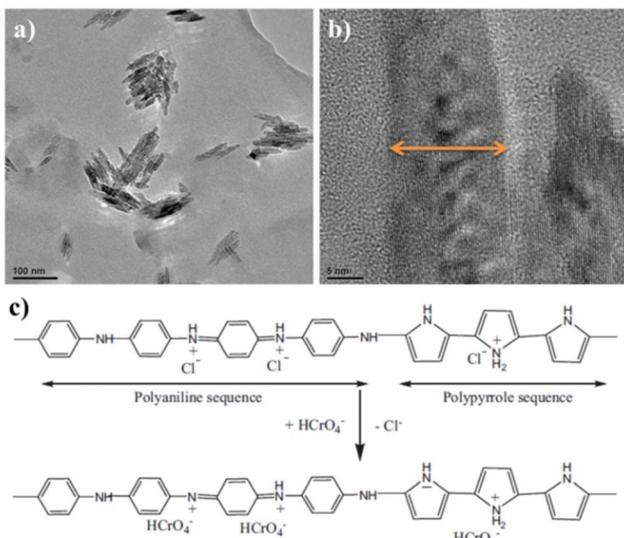
Fig. 4 (a) and (b) High-resolution TEM images of the PPy-PANI nanofibers at two different magnifications. (c) Plausible pathway to remove Cr(VI) from aqueous solutions using the PPy-PANI nanofibers. Reproduced with permission from ref. 68. Copyright 2012 Elsevier.

components of AC/PPSU/PEI/PEG at 0.25/35/5/6 wt%.[71] However, no reports on the application of such AC/polymer composites on heavy metal ion removal were available.

Due to the inert property of the carbon matrix, most of the polymer/carbon material composites are non-covalent, while in our previous research, we firstly synthesized carboxymethyl-cellulose (CMC)/CS grafted MWCNTs by a N_2-plasma-induced grafting technique.[20,73] The resulting CMC grafted MWCNT (MWCNT-*g*-CMC) was applied in U(VI) removal from wastewater solutions, and the results showed that the sorption percentage of U(VI) increased from 23% to 98% with the increase in MWCNT-*g*-CMC content from 0.1 g L^{-1} to 1.0 g L^{-1}, whereas the sorption percentage of U(VI) increased only from ∼8% to ∼19% on raw MWCNTs. U(VI) sorption on MWCNT-*g*-CMC was found to increase with increasing pH in acidic solution and decreased with increasing ionic strength at low $NaClO_4$ concentrations.[20] The prepared MWCNT-*g*-CS were also used to remove U(VI), Cu(II), and Pb(II) metal ions from large volumes of aqueous solutions, and the results showed that MWCNT-*g*-CS had much higher sorption capacity than MWCNTs, further demonstrating the possibility of applying such grafted MWCNTs-polymer composites in the solidification and pre-concentration of metal ions from large volumes of waste-water.[73] In the recent work from Nyairo *et al.*, PPy coated oxi-dized MWCNTs (oMWCNT/PPy) were applied to remove Pb(II) and Cu(II) from wastewater solutions, and achieved the sorp-tion maximum capacities of 26.32 and 24.39 mg g^{-1}, respect-ively, and a stable performance for at least five cycles.[74]

Compared with AC and CNTs, graphene, especially GO, is more widely used in polymers for improving the performance of heavy metal ion removal due to the presence of abundant functional surface groups, high surface areas and high water solubility.[72] For example, GO has been widely combined with chitosan, a natural aminopolysaccharide to form hydrogel composites.[75–78] He *et al.* synthesized porous GO/chitosan (PGOC) material, and the incorporation of GO increased the compressive strength of PGOC significantly. When 5 wt% GO was incorporated, the sorption capacity of Pb^{2+} increased ∼31% (up to 99 mg g^{-1}).[76] A magnetic cyclodextrin–chitosan/ GO (CCGO) composite prepared by Li *et al.*[78] exhibited better Cr(VI) removal efficiency at low pH. Due to the advantage of abundant amino and hydroxyl groups, high surface area, and the magnetic properties, the Cr(VI) can be easily and rapidly extracted from water. The adsorption kinetics followed the pseudo-second-order model, and the equilibrium data were well fitted by the Langmuir isotherm model. The speculated removal mechanism consists of four steps as follows: (1) Cr(VI) binding to CCGO through electrostatic interactions between protonated amine groups of CCGO and negatively charged Cr(VI) species. (2) Cr(VI) reduction to Cr(III) with the assistance of π electrons on the CCGO carbocyclic six-membered ring. (3) Cr(III) species binding on CCGO through the electrostatic attraction between the negatively charged groups (COO^-) of CCGO and Cr(III) or Cr(III) species released into solution by electrostatic repulsion between the cationic Cr(III) ions and protonated amine groups. (4) Cyclodextrin can bind Cr(VI) and

Cr(III) in the cavities to form the stable guest–host inclusion complexes. Through the subsequent phosphorylation of the GO–chitosan composite, there was ultrafast uptake of U(VI) within 15 min, with the sorption maximum capacity of 779.44 mg g^{-1} at pH 5.0 and 293 K. Further investigation indi-cated that the high immobilization of U(VI) on GO–CS–P was mainly dominated by inner-sphere surface complexation plus minor surface reduction contribution.[79]

In addition, poly(*N*-vinylcarbazole) (PVK),[80] PPy,[19,28,81] β-cyclodextrin,[82] PANI,[83] and poly(acrylamide) (PAM)[84] com-posed polymer composites also showed effective removal per-formance for heavy metal ions. For instance, PANI and reduced GO (PANI/RGO) composites were utilized as the effective adsorbents for Hg(II) adsorption from aqueous solu-tions. The adsorption capacity of Hg(II) on PANI/RGO increased from 515.46 to 1000.00 mg g^{-1} compared with PANI. The presence of RGO improved the enhancement by 7 times in the specific surface area and sorption sites.[83] PAM and RGO composites (RGO/PAM) were synthesized by free-radical *in situ* polymerization. The heavy metal ion (Pb(II)) and the benzenoid compound (methylene blue, MB) were selectively adsorbed by the composites, and the sorption capacity of Pb(II) was as high as 1000 mg g^{-1}. The spontaneous and exothermic adsorption kinetics of Pb(II) to RGO/PAM were well fitted to pseudo-second-order model (Fig. 5).[84] In our group, PAM grafted GO (PAM/GO) was applied for the simultaneous removal of radio-nuclides such as Eu(III), U(VI) and Co(II). The results suggested that the radionuclide sorption to PAM/GO was a spontaneous and endothermic process. The sorption maximum capacities of Co(II), Eu(III) and U(VI) on PAM/GO were 1.621, 1.245 and 0.698 mmol g^{-1}, respectively at T = 295 K and pH = 5.0 ± 0.1, which were much higher than GO.[85]

An obvious feature of the mentioned GO–polymer compo-sites for heavy metal ion removal is the high sorption ability and fast sorption rate originating from the full interaction between the materials and metal ions in the aqueous solutions *via* the abundant surface functionalities and high surface areas, which are crucial for practical applications.

3.3. Removal of heavy metals over polymer/clay(mineral) composites

3.3.1. Polymer/SiO_2 composites. As a porous material, SiO_2 with high specific surface area and good mechanical pro-perties has been widely used as an adsorbent for heavy metal ions.[86] The combination with polymer was also popular due to the advantages/disadvantages between SiO_2 and polymers since SiO_2 is not suitable for chelating with metal ions but has good mechanical properties and high surface area, while poly-mers are usually abundant in surface chelating groups for adsorbates.[87] In earlier research, Ghoul *et al.*[88] investigated the decontamination of Cd(II), Zn(II), Ni(II) and Pb(II) solutions using two types of silica gels modified with poly(ethylene-imine) (PEI) as adsorbents, *i.e.* crosslinked silica/PEI and silica/ PEI. The results showed that the sorption capacities depended on pH, initial metal concentration and to some extent the nature of metal ions. The metal ions can be recovered from the
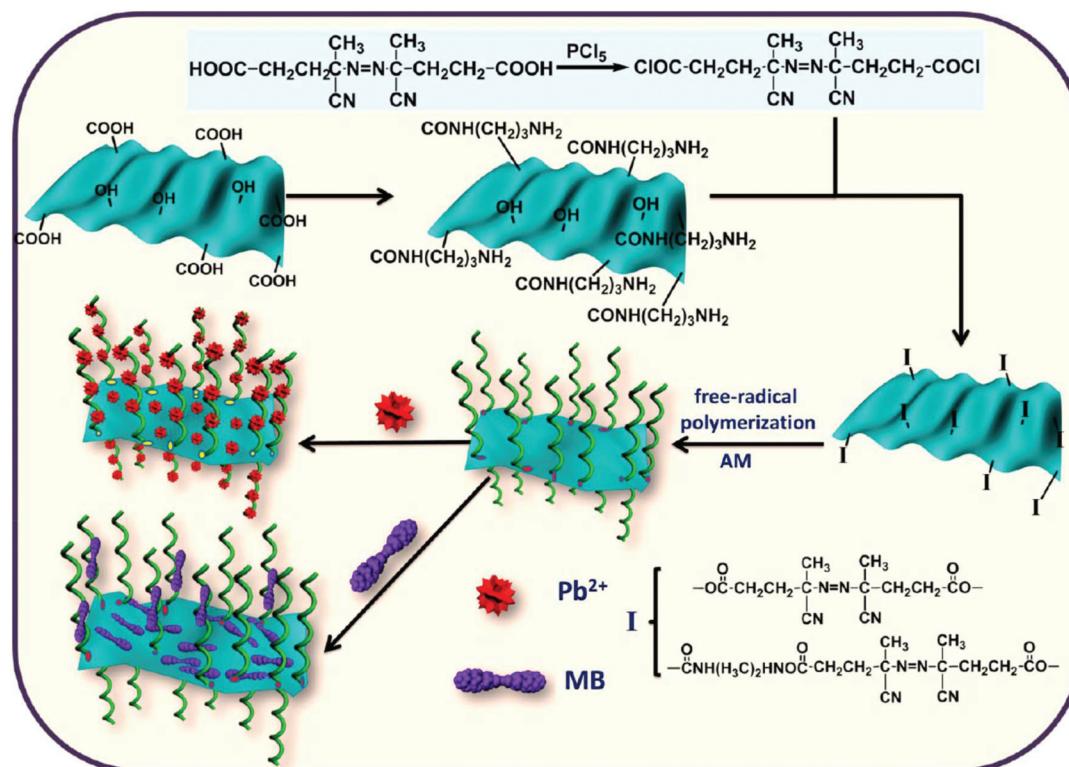
Fig. 5 Synthesis of PAM chains on RGO sheets, and Pb(II) and MB adsorption. Reproduced with permission from ref. 84. Copyright 2013 American Chemical Society.

adsorbents using dilute acid, but only on the crosslinked sorbents, and adsorbents can be regenerated and reused without sorption decrease. Other cations (such as Ca(II), Na(I)) and metals did not affect the sorption ability. Static tests also showed that (i) the saturation sorption capacities were higher for Zn(II) and Pb(II) than for Ni(II) and Cd(II) at pH = 6; (ii) the adsorption plateau was reached faster for Zn(II) and Pb(II) than for Ni(II) and Cd(II), and (iii) the selectivity of adsorption could be observed at pH > 5.[88] A novel composite material composed of silica gel microspheres encapsulated by imidazole functionalized polystyrene (SG-PS-azo-IM) was applied to investigate the removal of Ag(I), Ni(II), Cu(II), Hg(II), Zn(II), Pb(II), Pt(II), Mn(II), Pd(II), Fe(III), Cr(III) and Au(III) from wastewater solutions by Yin *et al.*[89] Results showed that SG-PS-azo-IM had the highest sorption capacity of 1.700 mmol g^{-1} for Au(III) calculated from the Langmuir model. This composite had excellent Au(III) adsorption properties in four solutions containing binary ions, especially in the systems of Cu(II)–Au(III) and Zn(II)–Au(III). In addition, Au(III) could be desorbed using an eluent solution of 0.5% thiourea and 1 mol L^{-1} HCl. This material could also quantitatively enrich Au(III) with the multiple enrichment of 5.28.[89] Another selective adsorption of heavy metal ions was found over poly(amidoxime)/SiO$_2$ (PAO/SiO$_2$).[90] Results showed that PAO/SiO$_2$ possessed strong chelating ability for heavy metal ions, with adsorption capacity towards Pb(II) and Cu(II) ions up to 12 g per 100 g and 10 g per 100 g, respectively. The endothermic chemical process dominated the entropy inter-

action, and increased with increasing temperature. The adsorption was dependent on pH. The PAO/SiO$_2$ had selectivity for heavy metal ions, with the sorption capacity in the order of Cd(II) < Pb(II) < Ni(II) < Cu(II).[90] Efficient and fast sorption of Pb(II) and Cu(II) was also found over mesoporous SBA-15-supported Pb(II)-imprinted polymers[91] and a thiol-functionalized mesoporous polyvinyl alcohol (PVA)/SiO$_2$ composite,[92] respectively. In particular, the adsorption capacity of poly(vinyl alcohol)/SiO$_2$ composite nanofibers towards Cu(II) was maintained even after six adsorption–desorption cycles (Fig. 6).[92]

Very recently, polyethylenimine(PEI)-tannins coated SiO$_2$ (SiO$_2$@PEI-TA) hybrids were synthesized *via* single-step multifunctional coating with PEI and tannins (TA).[93] Results showed that Cu(II) adsorption was fitted well to the Freundlich model with correlation coefficient of 0.9914, suggesting that the adsorption was mainly a heterogeneous process. Further thermodynamic analyses indicated that the interaction was actually endothermic and spontaneous, which may be due to the chemical interaction between Cu(II) ions and the functional groups (carboxyl and amine groups) on the surfaces.[93] Another new composite, *i.e.*, silica-sphere–poly(catechol hexamethylenediamine) (PCHA–SiO$_2$), was synthesized using a silica sphere as the hard template *via* the one-step facile polymerization of catechol and hexamethylenediamine. The PCHA–SiO$_2$ composite proved to be a very attractive adsorbent for Pb(II), Cu(II), and Cd(II) removal at low concentrations, with very good selective adsorption abilities for Cu(II) and Pb(II)
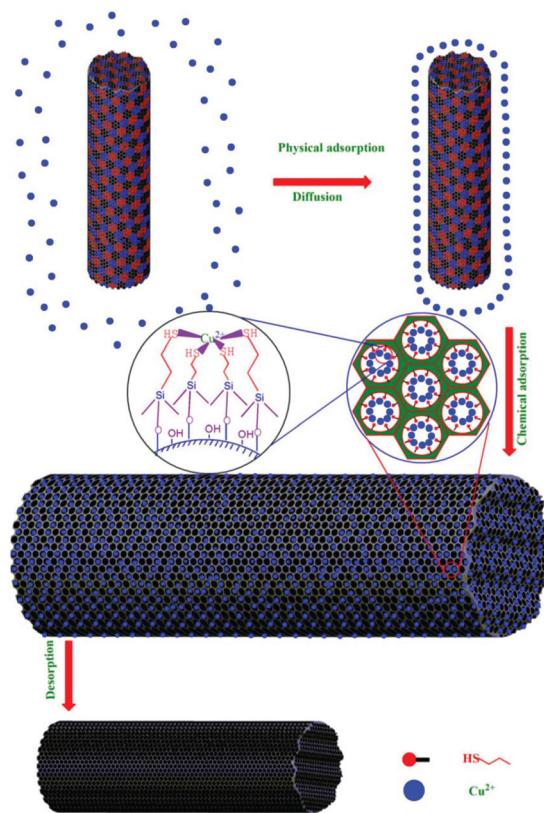
Fig. 6 The mechanism of Cu(II) adsorption on PVA/SiO$_2$ nanofibers. Reproduced with permission from ref. 92. Copyright 2010 Elsevier.

ions in a mixed solution containing these three ions at high concentrations, which was considered due to the reversible H$^+$ adsorption–desorption properties of the characteristic phenol amine structure on the surface.[94]

3.3.2. Polymer/phosphate composites. The ion exchange process is one of the most efficient approaches for metal ion adsorption, essentially driven by the coulombic or electrostatic interactions. Among the exploited inorganic ion exchanges, phosphates[95] such as zirconium phosphates, Ti(IV) arsenophosphate, and tungstomolybdophosphate have been widely used because of their fast kinetics, high capacity, and excellent thermal stability.[96] Unfortunately, phosphates are present as fine nanoparticles and cannot be directly employed in fixed-bed or any other flow-through systems because of the poor mechanical strength and excessive pressure drop. To overcome these difficulties, such phosphate nanoparticles have been composed within different porous polymers to obtain hybrids and facilitate their application.[97–99]

For example, Zhang et al.[46] fabricated three nanocomposites (ZrP–Cl, ZrP–S and ZrP–N) by the encapsulation of zirconium phosphate nanoparticles (nano-ZrP) within three macroporous polystyrene resins containing different surface groups (i.e., –SO$_3^-$, –CH$_2$Cl and –CH$_2$N$^+$(CH$_3$)$_3$) for Pb(II) removal. Results showed that the functional charged groups (–CH$_2$N$^+$(CH$_3$)$_3$ and –SO$_3^-$) were more beneficial than the neutral –CH$_2$Cl functional group to improve the dispersion of

nano-ZrP. The ZrP–S and ZrP–P showed higher capacity for Pb(II) removal than ZrP–Cl. As a result of the potential Donnan membrane effect, ZrP–S exhibited higher adsorption toward Pb(II) ion at high calcium levels as compared to ZrP–N. In addition, the resulting nanocomposites showed reinforced compressive strength compared with nano-ZrP.[46] As reported by Bushra et al.,[100] a novel PANI-based cation exchange composite containing Ti(IV) arsenophosphate has been synthesized by a simple chemical route. The sorption of different metal ions on the composite was performed using columns of this exchanger, significant separations of metal ions were achieved from the synthetic mixtures as well as tap water samples containing Cd(II), Pb(II), Zn(II), Fe(III) and Cr(IV) ions on the basis of high K_d values.[100]

Another Th(IV) polymer tungstomolybdophosphate (PANI/TWMP) composite was prepared via the sol–gel technique by mixing polyaniline with the precipitate of Th(IV) TWMP (Fig. 7).[53] The study revealed that compared to the inorganic counterpart (i.e., TWMP) and organic counterpart (i.e., PANI), the PANI/TWMP composite had much higher ion exchangeability (1.07 meq. g^{-1}). The PANI/TWMP was thermally stable and even retained the ion exchange capacity of 53.27% up to 400 °C. The selectivity studies indicated that the binary separations were also achieved. Cu(II) and Pb(II) ions were also effectively separated by PANI/TWMP from synthetic solutions.[53]

3.3.3. Polymer/clay composites. Natural clay materials such as montmorillonite, kaolinite, and bentonite, have attracted much interest for heavy metal ion removal because of the lamellar structure, availability, low cost, mechanical and chemical stability, non-toxicity and high cation exchange capacity. Nevertheless, such stacked lamellar structures result in many inaccessible sites and low surface area. The modification of clay materials with polymers with the intention of intercalating polymers or exfoliating the clay sheets for more exposed accessible sites provides good dispersion for overcoming the drawback.[101] The electrostatic interactions between polymers and the negatively-charged surface of layered clay minerals resulted in the formation of nanocomposites and the good dispersion. For example, the amidoxime functionalized organobentonite/polyacrylonitrile composite was synthesized via in situ intercalation polymerization and applied as an adsorbent for Zn(II), Cu(II), and Cd(II) ions. It provided
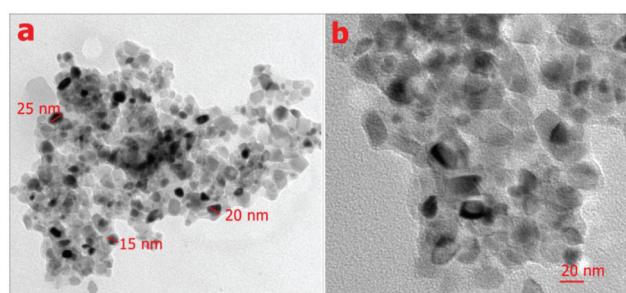

Fig. 7 TEM images of the PANI/tungstomolybdophosphate composite. Reproduced with permission from ref. 53. Copyright 2014 Elsevier.

maximum removal of 99.8% for Cu(II), 97.4% for Cd(II) and 98.9% for Zn(II) with 2 g L^{-1} of solid content at pH 6.0 and initial concentration of 25 mg L^{-1}. The monolayer adsorption maximum capacities calculated from the Langmuir model were 77.43 mg g^{-1} for Cu(II), 65.40 mg g^{-1} for Zn(II) and 52.61 mg g^{-1} for Cd(II) at 30 °C. Mechanistic investigation showed that the sorption process involved surface complexation, adsorption, in addition to ion exchange.[47] Similarly, other polymers, like polyacrylamide[12,102] and polymethacrylic acid (PMAA)[103] were also combined with bentonite for the efficient removal of Pb(II), Cu(II), Cd(II) and Hg(II).

Exfoliated PPy-organically modified montmorillonite (PPy-OMMTNC) was prepared *via* the *in situ* polymerization of pyrrole monomer. The rapid adsorption of Cr(VI) over the composite was spontaneous in nature and favored the increase of temperature at pH = 2.0. Kinetic data were well fitted to the pseudo-second-order model and the equilibrium data were well described using the Langmuir model, with maximum adsorption capacities of Cr(VI) of 112.3 mg g^{-1} at 292 K, 119.34 mg g^{-1} at 292 K, and 209.6 mg g^{-1} at 308 K and 318 K at pH = 2.0. The selective Cr(VI) adsorption was demonstrated with co-existing ions. The adsorbents can be used for three consecutive sorption–desorption cycles without any loss of its original sorption capacity.[104] Other polymer-based composites composed of montmorillonite such as chitosan–montmorillonite,[105,106] polyethylenimine–montmorillonite[107] have been applied to remove Cr(VI) and Se(IV) from water at extra-low concentrations. A typical montmorillonite/chitosan composite and the interaction between Cr(VI) and the composites are shown in Fig. 8.[108] More composites based on chitosan and perlite were also demonstrated for the efficient elimination of Cu(II),[109] Cd(II),[110] and Ni(II).[111]

3.3.4. Polymer/other metal oxide composites. Although metal oxides are not as widely used as the abovementioned

counterparts, there are still some kinds of metal oxides that cooperate with polymers for water remediation, such as SnO$_2$,[55] and TiO$_2$.[112] For example, the starch/SnO$_2$ nanocomposite was applied for Hg(II) removal from aqueous solutions. The experimental results showed that the maximum adsorption was achieved to be 192 mg g^{-1} at 25 °C and pH = 6, and equilibrium was achieved within 60 min. Further results demonstrated the spontaneous and endothermic process in nature. The sorption efficiency was still maintained at 94% after four adsorption–desorption cycles.[55] A recent report from Fallah *et al.* showed that a new biocompatible cellulose-titania-based nanocomposite (Cell-Com) was applied for the removal of Cd(II), Pb(II) and Zn(II) ions from solutions. At pH 7.0, the adsorption capacities of Cell-Com composites were 102.04 mg g^{-1} for Zn^{2+}, 102.05 mg g^{-1} for Cd^{2+} and 120.48 mg g^{-1} for Pb^{2+} after the contact time of 60 min at 298 K. The synthesized nanocomposite also showed interference resistance from coexisting ions and high selectivity for the sorption of Pb^{2+} ions. The Cell-Com can be easily regenerated and used without any significant loss of sorption capacity after 4–5 adsorption–desorption recycles in HCl or EDTA solution.[112] Our group also prepared a core–shell PANI/hydrogen-titanate nanobelt (PANI/H-TNB) composite, which had excellent sorption capacity towards Cr(VI) (156.94 mg g^{-1}) *via* a combination of chemical sorption and Cr(VI) reduction to Cr(III).[113]

3.4. Removal of heavy metals over polymer/metal composites

Metal nanoparticles are considered superior materials for chemistry and material science due to their remarkable catalytic and reduction ability.[21] In the field of wastewater treatment, considerable research has been focused on applying metal nanoparticles for high-valence heavy metal removal *via* reduction processes.[114–120] Although such metal nanoparticles are non-toxic to the environment, an obvious disadvantage lies
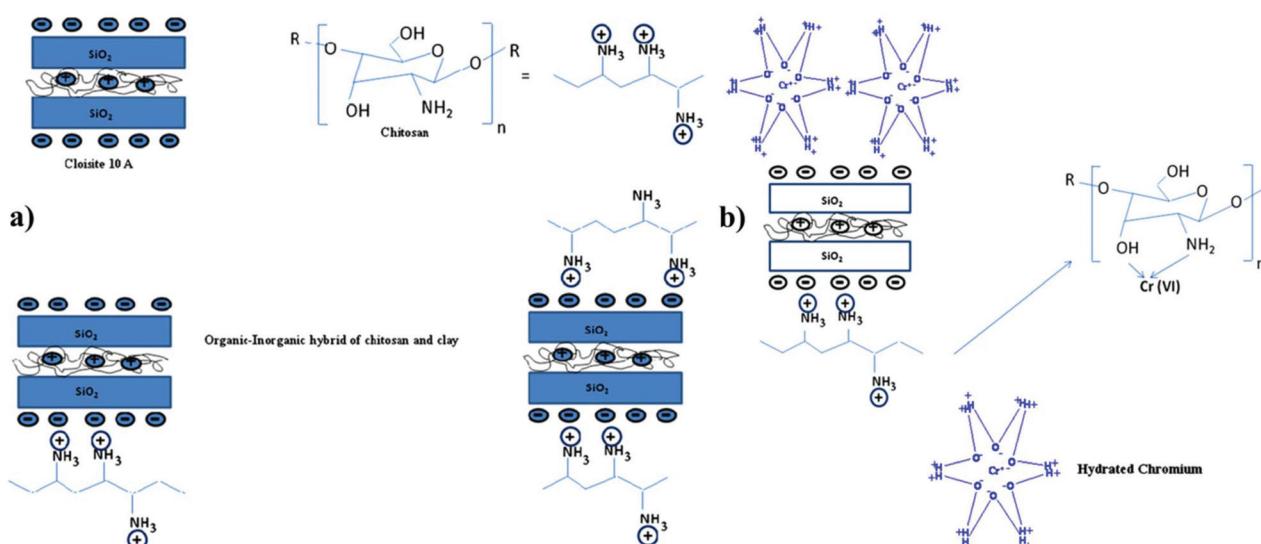
Fig. 8 (a) Organic−inorganic hybrid of chitosan and clay; (b) possible interaction mechanism of Cr(VI) with chitosan and organoclay. Reproduced with permission from ref. 108. Copyright 2011 Elsevier.

in its oxidation in air and the nanoscaled particles generally tend toward agglomeration, both of which seriously limit the inherent reducing specificity. Moreover, the risk of nanoparticles to the health and human beings has not been determined, and it is not easy to recycle the nanoparticles. To overcome such limitations, many studies have been focused on the immobilization of metal nanoparticles onto various supports like carbon materials,[121] clays[122] and polymers.[123–125]

The polymer-supported metal composites with large specific surface area have proven to be promising stabilizers for metal nanoparticles. Due to the elemental abundance and the inherent magnetism, zero-valent iron has drawn the most attention among all the metal nanoparticles.[126,127] Zhao et al. fabricated nanoscale Fe^0 with PVA as support and evaluated the Sb(III) and Sb(v) removal from water. Results showed that antimony adsorption was rapid and followed a pseudo-second rate law. The maximum adsorption capacities of granular PVA–Fe^0 for Sb(III) and Sb(v) were 6.99 and 1.65 mg g^{-1}, respectively. The antimony uptake mechanism by PVA–Fe0 was described as follows: Fe^0 was present in an acetalized PVA matrix before adsorption, which had been converted into magnetite (Fe_3O_4) after Sb(III) and Sb(v) adsorption. The Sb ions can promote Fe^0 oxidation. FTIR analyses indicated the magnetite's chemical binding to Sb(III) and Sb(v) after adsorption.[124] According to Bhaumik et al.,[43] metallic iron nanoparticles supported on PANI nanofibers were prepared simply at room temperature. The composite fibers were 80–150 nm in diameter, exhibiting ferromagnetic behavior, rapidly and efficiently removing As(v) and Cr(vi), with high capacities of 42.37 mg g^{-1} and 434.78 mg g^{-1}, respectively.[43] Highly efficient Cr(vi) reduction was also reported by Wang et al.[123] The CMC-stabilized Fe^0 nanoparticles displayed much less agglomeration but much Cr(vi) reduction as compared with those without a stabilizer. At a dose of 0.15 g L^{-1}, 100% of 10 mg L^{-1} Cr(vi) can be reduced in minutes. Analysis suggested that iron hydroxide and chromium hydroxide should be the final predominant products in this process.[123] In the latest report, Ravikumar et al. introduced a polymer-nZVI-based composite film prepared by the layer-by-layer coating of chitosan, polyethylene glycol blend, poly(sodium 4-styrene sulphonate) solution, and nZVI on a glass slide. The Cr(vi) sorption capacity of 394 mg g^{-1} was achieved at optimized conditions using Response Surface Methodology (RSM), with the reduction and binding of Cr(vi) on the polymer-nZVI-based film and SRB biomass.[128]

Although copper nanoparticles are relatively less investigated, Wu et al. used the ionotropic crosslinking to fabricate chitosan-tripolyphosphate chelating beads, which were further used to fabricate the zero-valent copper-chitosan composites. The resulting nanoparticles were well dispersed on the chitosan-tripolyphosphate beads, with maintained and appropriate dispersion and stability. The results showed that the fabricated nanocomposites displayed higher adsorption capacity for Cr(vi) than the chitosan-tripolyphosphate beads. Surface sorption, precipitation and reduction were

considered the important mechanisms for chromium remediation.[129]

3.5. Removal of heavy metals over magnetic polymer composites

As mentioned above, various polymer composites have been synthesized for heavy metal ions' removal with high adsorption capacities, fast adsorption kinetics and stability. However, for practical applications, separating adsorbents from the aqueous solution with low cost is also one important factor. Traditional separation techniques such as sedimentation and filtration have disadvantages such as the time-cost and the filter blocking. In addition, the adsorbents may be discarded with the process sludge, generating secondary pollution. With the development of magnetic separation, incorporating magnetic nanoparticles into the polymer matrix has attracted much attention.[130] To date, natural polymers like chitosan,[131] cyclodextrin polymer,[57,132] artificial polymers like polystyrene,[133] PPy,[134,135] poly(1-vinylimidazole)[136] have been involved in magnetic polymer composites for heavy metal ion removal.

Generally, magnetic particles that are very active and easily oxidized in air, lose some of their magnetism and dispersibility. When coating such magnetic nanoparticles with polymers, the toxicity is reduced, aggregation is inhibited, and the storage life is extended. Moreover, the abundant surface groups on polymers make further functionalization of such composites feasible, resulting in ternary composites.[137] The major magnetic particles embedded into polymers include Fe_3O_4,[138,139] Fe_2O_3,[140] $CoFe_2O_4$,[138,141] $NiFe_2O_4$,[142,143] and $ZnFe_2O_4$.[144] In general, the resulting magnetic polymer composites have two kinds of structures: magnetic core-polymer shell and homogeneous magnetic cores dispersed in the polymer matrix.[130] As a typical example, chitosan magnetic composites were synthesized from the amine-functionalized magnetite nanoparticles, which were conveniently removed from water under an external magnet. The magnetic nanoparticles were applied to eliminate metal ions from water based on the fact that the chitosan was inactive on the magnetic nanoparticle surface and can be coordinated with metal ions. Results indicated that the interaction between heavy metal ions and chitosan was reversible, and the metal ions were desorbed from chitosan in weak acidic conditions with the assistance of ultrasound radiation.[145] The magnetic chitosan composites have also been further modified to enhance the performance. Zhou et al. prepared chitosan magnetic microspheres and further modified them with thiourea for the elimination of metal ions. The adsorption properties of the resulting thiourea towards Cu(II), Hg(II), and Ni(II) ions showed that the adsorption kinetics of all systems followed the pseudo-second-order equation, indicating chemical sorption as the rate-limiting step, without involving a mass transfer in solution. The maximum adsorption capacities were 625.2 mg g^{-1} for Hg(II), 66.7 mg g^{-1} for Cu(II), and 15.3 mg g^{-1} for Ni(II) ions, as given by the Langmuir isotherm. Thiourea displayed higher sorption ability for Hg(II) at all experimental conditions studied. The sorption

activity decreased with the increase in temperature. The metal ion-loaded thiourea could be regenerated with an efficiency of >88% using 0.01–0.1 M EDTA.[146]

Cyclodextrin-based magnetic composites were often used in water remediation. For instance, carboxymethyl-β-cyclodextrin (CM-β-CD) polymer modified Fe_3O_4 (CDpoly-MNPs) nanoparticles were fabricated for the selective removal of Cd(II), Pb(II), and Ni(II) ions from solution. The adsorption was found to be dependent on ionic strength, pH, and temperature. A period of 45 min was enough to achieve equilibrium, and non-competitive adsorption mode maximum uptakes for Cd(II), Pb(II) and Ni(II) were 27.7, 64.5 and 13.2 mg g^{-1}, respectively at T = 25 °C, with adsorption isotherms fitted well by the Langmuir isotherm and kinetic process simulated by the pseudo-second-order model. Due to the complexation abilities of metal ions with the multiple carboxyl and hydroxyl groups in polymer backbone, the composites showed enhanced adsorption capacity. CDpoly-MNPs preferentially adsorbed metal ions with the affinity order of Ni(II) < Cd(II) ≪ Pb(II) in competitive adsorption experiments, which was explained by the hard–soft acid and base (HSAB) theory.[132] In our research group, cyclodextrin was also embedded with magnetic nanoparticles for the elimination of U(VI)[147] and Cu(II).[148] Batch experiments suggested an optimal pH value of 7.0 for CD/HNT/Fe_3O_4 in U(VI) decontamination from solutions.[147] The irreversible sorption was attributed to the inner-sphere binding of U(VI) on the surface sites. The sorption capacity of U(VI) on CD/HNT/Fe_3O_4 was 4.52×10^{-4} mol g^{-1} (pH = 5.5 and T = 298 K).[147] We also found that the β-CD grafted Fe_3O_4 particles showed an enhanced sorption capacity because of the strong abilities of multiple hydroxyl groups and the inner cores of the hydrophobic cavity in β-CD to form strong complexes with metal ions like Cu(II).[148] The ternary magnetic poly(acrylamide)-stabilized FeS/Fe_3O_4 (PAAM–FeS/Fe_3O_4) composite was proven to be a suitable adsorbent for the selective preconcentration of U(VI) from solution, with a maximum enrichment capacity of 311 mg g^{-1} at pH = 5.0 and 20 °C due to the fact that both amide groups and FeS on PAAM–FeS/Fe_3O_4 surfaces have strong chemical affinities for U(VI), and FeS could also effectively reduce U(VI) to U(IV).[149]

PPy containing magnetic composites were proven to be quite efficient at Cr(VI) removal. Bhaumik et al. found that up to 100% adsorption onto the Fe_3O_4 coated PPy magnetic nanocomposite at Cr(VI) concentration of 200 mg L^{-1} at pH 2, and Cr(VI) removal was decreased with the increase in pH. Further studies suggested that ion exchange and reduction were the possible mechanisms of Cr(VI) removal.[135] Combined with graphene oxide, a novel ternary magnetic composite consisting of PPy, Fe_3O_4 nanoparticles and rGO, (PPy–Fe_3O_4/rGO) was prepared by a facile two-step route. Characterization analysis showed the successful decoration of chain-like PPy on Fe_3O_4/rGO. The ternary PPy–Fe_3O_4/rGO showed excellent performance for Cr(VI) removal (293.3 mg g^{-1}), much higher than Fe_3O_4/rGO. The removal process was exothermic, spontaneous and pH dependent. Cr(VI) ions were adsorbed through electro-static attraction and ion exchange. Similarly, the nitrogen species of Ppy could also reduce Cr(VI) to low-toxicity Cr(III).[137]

Other polymers like polycaprolactone,[56] 2,3-diaminophenol and formaldehyde (DAPF)-based polymer[38] and poly(L-vinylimidazole)[136] were also demonstrated to be efficient for the removal of heavy metal ions such as As(III), Pb(II) and Cu(II). Particularly, the poly(L-vinylimidazole)-grafted magnetic nanoparticles showed the selective sorption of divalent metal ions with an order of Co(II) < Ni(II) ≪ Cu(II). The maximum capacity of Cu(II) adsorption was 0.11 mmol g^{-1} at pH = 5.3. Selective separation and recovery of Cu(II) from Co(II)/Cu(II) mixture solution was demonstrated over the pH range of 3 to 7.[136]

4. Adsorption analysis of heavy metal ions onto polymer-based composites

4.1. Macro analysis

For primary and direct research, the adsorption process can be studied by batch experiment, through which the effect of pH, kinetics, thermodynamics and the adsorption capacity can be determined.

4.1.1. Effect of pH. In the adsorption process, the pH of the solution is vital to the surface protonation of the adsorbent and species distribution of the target metal ion, thus significantly affecting the adsorption behavior. For each specific heavy metal ion, the optimum pH value is dependent on polymer composites. Due to the existence of various functional groups such as –NH$_2$, –COOH, –OH, etc., most of such functional groups are protonated and positively charged at lower pH, while at higher pH, they are deprotonated and negatively charged. Moreover, the H$^+$ and OH$^-$ in solution may compete in the adsorption. For Cu(II), Ni(II), Zn(II), Cd(II) and Hg(II), the adsorption on polymer composites usually increases with increasing pH values,[146,150] while for Cr(VI), a gradual decrease in Cr(VI) removal efficiency is observed with the increase of pH due to different predominant species of Cr(VI) at different pH values. At low pH, the positively charged surface displayed increasing affinity for the negatively charged HCrO$_4^-$ and Cr$_2$O$_7^{2-}$ anions. Furthermore, the increased removal efficiency is also related to the anion exchange property of the PPy by replacing the doped Cl$^-$ with either HCrO$_4^-$ or Cr$_2$O$_7^{2-}$; at high pH, more OH$^-$ in solution would compete with CrO$_4^{2-}$ for the adsorbent active sites.[104]

To determine the ideal pH value for optimized adsorption, the point of zero charge (pH$_{PZC}$) was determined. At pH < pH$_{PZC}$, the surface of adsorbents is positively charged and thus the anions like Cr$_2$O$_7^{2-}$ would be adsorbed on the positively charged surface. At pH higher than the pH$_{pzc}$, the adsorbent surface is negatively charged and thereby the anions would be difficult to adsorb due to the electrostatic repulsion.

4.1.2. Adsorption kinetics. The kinetics in the adsorption process is not only important for practical applications but also important to analyze the adsorption mechanism and deduce the possible rate-limiting step. The kinetics is dependent on the transfer rate of metal ions to the adsorbent

surface as well as the interaction between metal ions and the adsorbent surface. The kinetic investigation is mainly studied by the time-dependent adsorption behavior. In general, there are three types of kinetic models: (i) pseudo-first-order kinetic model; (ii) pseudo-second-order kinetic model, and (iii) intra-particle diffusion kinetic model.[130] As mentioned in section 3, almost all the adsorption kinetics of heavy metal ions onto the polymer-based composites were proven to fit the pseudo-second-order model,[65,67,68,70,78,84,104,124,132,146] which indicated that the rate-limiting step in the target metal ion removal onto the polymer composites involved chemisorption due to strong interaction, coordination, complexation, and/or chelation between sorbent and sorbate.[151] For instance, Yang *et al.* studied the adsorption kinetics of Pb(ɪɪ) onto RGO/PAM by fitting the kinetic data with both pseudo-first-order and pseudo-second-order models.[84] The value of the correlation coefficients (R^2) from the pseudo-second-order mode is relatively higher than that from the pseudo-first-order mode, suggesting the chemisorption process. In minor cases, intra-particle diffusion was included in the process. For example, the adsorption of Sr(ɪɪ) onto magnetic chitosan beads has been studied as reported by Chen and Wang.[152] It demonstrated that the kinetic data was well fitted by an intra-particle diffusion model, indicating that both external mass transfer and intra-particle diffusion were the rate controlling factors.

4.1.3.　**Effect of temperature.** The effect of temperature on the adsorption process is related to the thermodynamic parameters. Typically, there are two kinds of thermodynamic processes, namely, exothermic and endothermic processes. The apparent temperature effect is dependent on the adsorption process, which includes three steps: (i) the dissociation of metal ion from the initial hydrate states; (ii) the adsorption of the metal ion onto the adsorbents; (iii) the desorption of metal ions from the adsorbents. The first and third steps are endothermic while the second step is exothermic. If the interaction between metal ions and the adsorbents is high, the final process is exothermic; otherwise, the process is endothermic. Most of the adsorption is exothermic, which means that the adsorption decreases with the increase in temperature, such as the adsorption of Pb(ɪɪ) on rGO/poly (acrylamide) composites and Cr(ᴠɪ) adsorption on PPy decorated RGO–Fe_3O_4 composites.[84,137] Reports have also shown the endothermic adsorption process, such as Cu(ɪɪ) removal by magnetic chitosan nanoparticles[153] and Cr(ᴠɪ) removal by magnetic chitosan–iron(ɪɪɪ) hydrogel.[154]

4.1.4.　**Adsorption capacity evaluation.** The adsorption capacity is one of the most important factors to determine the performance of adsorbents. By using the convenient batch experimental technique, the maximum adsorption amount of adsorbate per mass of adsorbent can be obtained by simulating the resulting isotherm curves with different isotherm models, such as Langmuir, Freundlich, Dubinin–Radushkevich (D–R), Temkin and so on,[70,155] among which, the Langmuir and Freundlich models are the most often used.[132,135,148] Typically, the Langmuir model is often based on the formation of monolayer adsorption on the surface of

the adsorbents with a finite number of identical sites, which are homogeneously distributed on the surface. The Freundlich model assumes an exponentially decaying adsorption site energy distribution,[156] which was applied to describe the heterogeneous surface characterized by a heterogeneity factor of n. The D–R isotherm model is usually employed to determine the nature of chemical or physical biosorption processes.[157] The Temkin isotherm model is based on the assumption that (i) the adsorption heats of all molecules present in the layer linearly decrease with the coverage because of adsorbate–adsorbent interactions; (ii) a uniform distribution of binding energies is applied to characterize the adsorption.[158]

Regarding polymer-based composites, the adsorption isotherms were approximately fitted according to the Langmuir model. For example, the sorption capacity of UO_2^{2+} calculated from the Langmuir simulation was ~16.2 mg g^{-1} for MWCNTs but about 39.2 mg g^{-1} for chitosan modified MWCNTs.[73] Li *et al.* demonstrated that the adsorption isotherms of Cu(ɪɪ) on magnetic polymer composites can be better fitted by the Langmuir isotherm model than by the Freundlich isotherm model, suggesting a monolayer coverage of Cu(ɪɪ).[148] In an unusual case as reported by Huang *et al.*, the equilibrium data of Cu(ɪɪ) adsorption on polyethylenimine-tannins coated SiO_2 hybrids was better fitted with the Freundlich model with the correlation coefficient of 0.9914, suggesting that Cu(ɪɪ) adsorption was mainly a heterogeneous adsorption process. For better comparison between different kinds of polymer-based composites, the reported adsorption capacities towards heavy metal ions have been summarized and tabulated in Table 1. The performances of other typical adsorbents without polymer-counterparts are also listed in the table for the readers' information. More related comparisons for these adsorbents can be found in the previous reviews and the references in the reviews.[26,27] It is obviously noted that polymer-based composites exhibit higher adsorption capacity than other conventional adsorbents.

4.2.　Micro analysis

For deeper insight into the adsorption process, more advanced analysis techniques such as spectroscopic techniques, theoretical calculation and simulation have been applied in order to clarify the mechanisms, which generally include physical adsorption, chemical bonding (complexation and/or chelation), ion exchange, *etc.* For the polymer-based adsorbents, the multiple components also lead to more complex mechanisms that are often influenced by a wide range of factors like functional groups on the composites, the structure of the composites and the adsorption environment.

4.2.1.　**X-ray photoelectron spectroscopy (XPS) analysis.** XPS is a powerful technique that provides information on the state of the metal species on the solid surface. Adsorbents with adsorbed heavy metal ions often show quite different XPS spectra due to the interaction of metal ions with the surface functional groups.[55,159] Typically, Shao *et al.* found that the deconvolution of the Cu 2p and Pb 4f XPS spectra of adsorbed

Table 1 Reported adsorption capacities towards heavy metal ions by polymer-based composites and typical adsorbents without polymer counterparts

Polymer-based composites	Targets	Concentration	pH	T (K)	Adsorption capacity	Ref.
Carboxymethyl cellulose/chitosan grafted MWCNTs	UO_2^{2+}	0.2 mmol L^{-1}	5.0	298	4.7×10^{-4} mol g^{-1}	20
PMMA/PEI core/shell nanoparticles	Cu(II)	—	5.0	298	14 mg g^{-1}	37
Metallic iron nanoparticles–PANI composite	As(V)	5–100 mg L^{-1}	7.0	298	42.37 mg g^{-1}	43
Metallic iron nanoparticles–PANI composite	Cr(VI)	75–250 mg L^{-1}	2.0	298	434.78 mg g^{-1}	43
Starch/SnO$_2$ nanocomposite	Hg(II)	10–150 mg L^{-1}	6.0	298	192 mg g^{-1}	55
PANI/PPy copolymer nanofibers	Co(II)	100 to 500 mg L^{-1}	—	298	185.18 mg g^{-1}	65
Mesoporous silica with PANI/PPy nanoparticles	Cd(II)	50–350 mg L^{-1}	—	298	384.615 mg g^{-1}	66
Polyacrylonitrile/PPy core/shell nanofiber	Cr(VI)	30 to 200 mg L^{-1}	2.0	298	61.80 mg g^{-1}	67
PPy-PANI nanofibers	Cr(VI)	100 to 400 mg L^{-1}	2.0	298	227 mg g^{-1}	68
PEDOT/PSS-lignin composites	Pb(II)	—	—	298	452.8 mg g^{-1}	69
Chitosan/PAA magnetic composite microspheres	Cu(II)	20 to 400 mg L^{-1}	5.5	298	174 mg g^{-1}	70
oMWCNT/PPy	Pb(II)	10–100 mg L^{-1}	6.0	298	26.32 mg g^{-1}	74
oMWCNT/PPy	Cu(II)	10–100 mg L^{-1}	5.0	298	24.39 mg g^{-1}	74
Magnetic cyclodextrin–chitosan/GO	Cr(VI)	50 mg L^{-1}	3.0	303	61.31 mg g^{-1}	78
PPy/GO	Cr(VI)	—	—	—	9.56 mmol g^{-1}	28
PANI/rGO nanocomposite	Hg(II)	10–400 mg L^{-1}	4.0	298	1000.00 mg g^{-1}	83
Poly(ethyleneimine)-silica gels	Pb(II)	—	5.0–6.0	298	82.64 mg g^{-1}	88
Poly(ethyleneimine)-silica gels	Zn(II)	—	5.0–6.0	298	52.08 mg g^{-1}	88
Poly(ethyleneimine)-silica gels	Ni(II)	—	5.0–6.0	298	28.25 mg g^{-1}	88
Poly(ethyleneimine)-silica gels	Cd(II)	—	5.0–6.0	298	38.46 mg g^{-1}	88
Thiol-functionalized PVA/SiO$_2$ composite	Cu^{2+}	0.5–10 mmol L^{-1}	5.0	303	489.12 mg g^{-1}	92
SBA-15-supported Pb(II)-imprinted polymer	Pb(II)	—	6.0	288	42.55 mg g^{-1}	91
Polyethylenimine-tannins coated SiO$_2$ hybrid	Cu(II)	5–100 mg L^{-1}	7.0	298	100.1 mg g^{-1}	93
Polymer-supported zirconium phosphate	Pb(II)	40–150 mg L^{-1}	5.5	288	556 mg g^{-1}	98
Cellulose-sodium montmorillonite composite	Cr(VI)	—	5.0	298	22.2 mg g^{-1}	101
PMAA grafted chitosan-bentonite composite	Hg(II)	—	—	298	125 mg g^{-1}	103
PMAA grafted chitosan-bentonite composite	Pb(II)	—	—	298	111 mg g^{-1}	103
PPy-montmorillonite clay nanocomposite	Cr(VI)	250 to 800 mg L^{-1}	2.0	298	119.34 mg g^{-1}	104
Chitosan/cloisite nanocomposite	Cr(VI)	50–1000 mg L^{-1}	3.0	288	357.14 mg g^{-1}	108
Magnetite–polyethylenimine–montmorillonite	Cr(VI)	—	3.0	298	8.8 mg g^{-1}	107
Chitosan coated perlite beads	Cu(II)	50–4100 mg L^{-1}	4.5	298	104 mg g^{-1}	109
TiO$_2$-grafted cellulose	Zn^{2+}	20–80 ppm	7.0	298	102.04 mg g^{-1}	112
TiO$_2$-grafted cellulose	Cd^{2+}	20–80 ppm	7.0	298	102.05 mg g^{-1}	112
TiO$_2$-grafted cellulose	Pb^{2+}	20–80 ppm	7.0	298	120.48 mg g^{-1}	112
PANI coated protonic titanate nanobelt composites	Cr(VI)	—	5.0	298	156.94 mg g^{-1}	113
PVA-zero-valent iron composites	Sb(III)	0–20 mg L^{-1}	7.0	298	6.99 mg g^{-1}	124
PVA-zero-valent iron composites	Sb(V)	0–20 mg L^{-1}	7.0	298	1.65 mg g^{-1}	124
Polymer-zero valent iron-based composite film	Cr(VI)	10 to 50 mg L^{-1}	7.0	298	394 mg g^{-1}	128
Carboxymethyl-β-cyclodextrin modified Fe$_3$O$_4$	Pb^{2+}	50 to 400 mg L^{-1}	5.5	298	64.5 mg g^{-1}	132
Carboxymethyl-β-cyclodextrin modified Fe$_3$O$_4$	Cd^{2+}	50 to 400 mg L^{-1}	5.5	298	27.7 mg g^{-1}	132
Carboxymethyl-β-cyclodextrin modified Fe$_3$O$_4$	Ni^{2+}	50 to 400 mg L^{-1}	5.5	298	13.2 mg g^{-1}	132
PPy/Fe$_3$O$_4$ magnetic nanocomposite	Cr(VI)	200 to 600 mg L^{-1}	2.0	298	169.49 mg g^{-1}	135
PPy decorated rGO–Fe$_3$O$_4$ magnetic composites	Cr(VI)	48–250 mg L^{-1}	3.0	318	293.3 mg g^{-1}	137
PAM-stabilized FeS/Fe$_3$O$_4$	U(VI)	—	5.0	293	311 mg g^{-1}	149
Magnetic chitosan−iron(III) hydrogel	Cr(VI)	20 to 160 mg L^{-1}	3.0	303	144.9 mg g^{-1}	154
Pyromellitic acid dianhydride/phenylaminomethyl	Pb(II)	—	5.0	298	7.16 mmol g^{-1}	162
Pyromellitic acid dianhydride/phenylaminomethyl	Cu(II)	—	4.0	298	0.28 mmol g^{-1}	163
Poly(amidoamine) modified GO	Fe(III)	0.0193 mmol L^{-1}	—	298	0.5312 mmol g^{-1}	3
Poly(amidoamine) modified GO	Cr(III)	0.0193 mmol L^{-1}	—	298	0.0798 mmol g^{-1}	3
Poly(amidoamine) modified GO	Zn(II)	0.0193 mmol L^{-1}	—	298	0.2024 mmol g^{-1}	3
Poly(amidoamine) modified GO	Pb(II)	0.0193 mmol L^{-1}	—	298	0.0513 mmol g^{-1}	3
Poly(amidoamine) modified GO	Cu(II)	0.0193 mmol L^{-1}	—	298	0.1368 mmol g^{-1}	3
Poly(N-vinylcarbazole)–GO	Pb(II)	5–300 mg L^{-1}	7.0	298	982.86 mg g^{-1}	164
Chitosan/GO	Au(III)	80–500 mg L^{-1}	—	298	1076.649 mg g^{-1}	27
Chitosan/GO	Pd(II)	80–500 mg L^{-1}	—	298	216.92 mg g^{-1}	27
PPy–rGO	Hg(II)	50–250 mg L^{-1}	3.0	293	979.54 mg g^{-1}	26
PEI grafted magnetic porous adsorbent	Zn(II)	100 mg L^{-1}	6.5	298	138.8 mg g^{-1}	27
Poly(methacrylic acid) grafted-chitosan/bentonite	Th(IV)	100–500 mg L^{-1}	5.0	303	110.5 mg g^{-1}	29
Chitosan/clinoptilolite	Cu(II)	—	5.0	298	719.39 mg g^{-1}	152
Amino modified MWCNT	Pb(II)	5 mg L^{-1}	6.2	298	25.64 mg g^{-1}	162
Raw MWCNT	Pb(II)	5 mg L^{-1}	6.2	298	1.66 mg g^{-1}	162
Oxidised activatedcarbon	Pb(II)	10 to 150 mg L^{-1}	5.0	298	389 mg g^{-1}	163
Activated carbon/iron oxyhydroxide	arsenate	10 to 150 mg L^{-1}	6.0	298	32.86 mg g^{-1}	165
Supported nano Fe^0 on activated carbon	arsenate	—	6.5	298	12 mg g^{-1}	121
Hematite	Cu(II)	—	5.2	298	84.46 mg g^{-1}	166
TiO$_2$ nanoparticle	Pb(II)	—	8.0	298	81.3 mg g^{-1}	167
Bentonite supported iron oxide	Pb(II)	—	—	—	31.86 mg g^{-1}	168

Table 1 *(Contd.)*

Polymer-based composites	Targets	Concentration	pH	T (K)	Adsorption capacity	Ref.
Bentonite supported magnesium oxide	Cu(II)	—	—	—	58.44 mg g^{-1}	169
Pyrolised activated carbon	Hg	50–1000 mg L^{-1}	6.0	333	172.4 mg g^{-1}	170
Sawdust	Cd(II)	—	5.0	293	73.6 mg g^{-1}	171
Activated carbon coated with magnetite particles	Cr(VI)	100–1000 mg L^{-1}	2.0	300	57.37 mg g^{-1}	172

Cu^{2+} and Pb^{2+} on the chitosan modified MWCNTs indicated the interaction of these metal ions with the hydroxyl groups, carboxyl groups and other groups such as amino groups and acetyl groups.[73] Similar results have been reported in the literature.[38,145,159–161] For high-valance Cr(VI) removal, XPS was also used to confirm the reduction of Cr(VI) to Cr(III). Bhaumik *et al.* analyzed the PPy-PANI nanofibers after the adsorption of Cr(VI) by XPS. The binding energies at 577.5 eV and 587.2 eV are consistent with Cr(III) and Cr(VI), suggesting that adsorbed Cr(VI) on the surface of the nanofibers was partially reduced to Cr(III) by electron-rich polymeric moieties.[68] A similar mechanism was also reported by Wang *et al.*[137]

4.2.2. Fourier transform infrared (FTIR) spectroscopy. FTIR is another sensitive technique that can provide information about the adsorption states of the adsorbed heavy metal ions.[153] For instance, compared with the FTIR spectra of the PVA–Fe^0 adsorbent before and after reaction with either Sb(III) or Sb(V), three peaks at 662, 563 and 456 cm^{-1} were clearly observed after reaction with Sb(III) or Sb(V). The peak at 662 cm^{-1} could be assigned to the Fe–O–H bending mode of magnetite, indicating the presence of active magnetite and interactions between Fe–O bonds with Sb(III) or Sb(V). The two bands at 563 cm^{-1} and 456 cm^{-1} have been assigned to the Sb–O–Sb symmetric stretching vibrations and bending vibrations, respectively.[124] Setshedi *et al.* found that all the organic FTIR peaks in the polymer composites (PPy-OMMT NC3) shifted to increasing wavenumber after Cr(VI) adsorption, indicating a possible interaction between Ppy-OMMT NC3 and Cr(VI) ions. This may be due to the p electrons of the polymer backbone interacting with the doping ions of various types of dopants, which possibly agitates the PPy conjugate structure, thus limiting the extent of charge delocalization of the polymer chain, followed by adsorption frequency redshifts.[104] According to Kumar *et al.*, hydrogen bonding interactions were also probable between the oxygen atoms in the bichromate anion and the hydroxyl protons in cellulose from FTIR results.[101] From the FTIR measurement, Chen and Wang[152] reported that the adsorption of Sr(II) onto magnetic chitosan beads was mainly attributed to the amine groups. Similarly, Chen *et al.*,[153] used FTIR to show the binding of Cu(II) ions through the NH$_2$ and OH groups in chitosan.

4.2.3. (Extended) X-ray absorption (fine) structure spectroscopy (EXAFS/XAS). Based on the advances of synchrotron-based X-ray absorption spectroscopy (XAS) and extended X-ray absorption fine structure (EXAFS) spectroscopy for important innovations, these techniques have also been widely used as a very powerful technique to describe the local environment of a target metal ion on the surface of polymers,[173] clays,[174] gra-

phene materials,[159,175–177] carbonaceous canofibers.[173] For example, according to the fitting of EXAFS spectra, the U–Fe (at ~3.2 Å) and U–C (at ~2.9 Å) shells were observed in the U(VI) adsorbed nZVI/rGO composites, indicating the formation of inner-sphere complexes on nZVI/rGO surfaces, as shown in Fig. 9.[174] It was also found from EXAFS analysis that the significant splitting of the equatorial oxygen (U–Oeq) shell was attributed to the electron scattering of the elemental sulfur in the highly effective enrichment of U(VI) on sulfonated GO at ultralow pH.[178] However, it is difficult to find out such investigations on the polymer-based composites for heavy metal ion removal. It is highly encouraged that in future studies, XAS and EXAFS should be taken into account as a useful technique for clearer mechanism exploration.

4.2.4. Theoretical calculation. In order to obtain greater theoretical understanding of the interaction between heavy metal ions and the adsorbents, density functional theory (DTF) and molecular simulation have been utilized from a viewpoint of calculation chemistry.[157,158,160,161] The advantage of theoretical calculations is to get some information such as binding energy, bond distance, kinetic process *etc.*, which are crucial to understanding the interaction mechanism at the molecular level. This information is difficult to achieve from experiments. For instance, in the theoretical calculations for U(VI) adsorption on sulfonated GO, the energy of uranyl-carboxyl (−3198.498 Hartree/particle) was higher than that of the uranyl-sulfonyl (−3198.511 Hartree/particle) at pH 2.0,
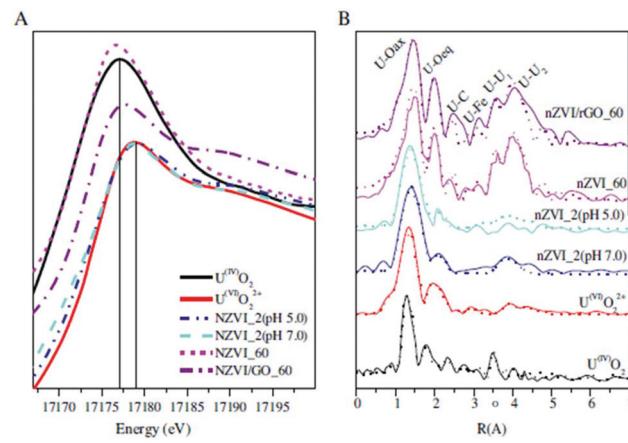

Fig. 9 XANES spectra (A) and Fourier transform (FT) of EXAFS spectra (B, solid and dashed lines: experimental and fitted data) for reference samples and U(VI)-reacted nZVI and nZVI/rGO composites, T = 25 ± 1 °C, I = 0.01 mol L^{-1} NaClO$_4$ pH = 5.0. Reproduced with permission from ref. 174. Copyright 2014 Elsevier.
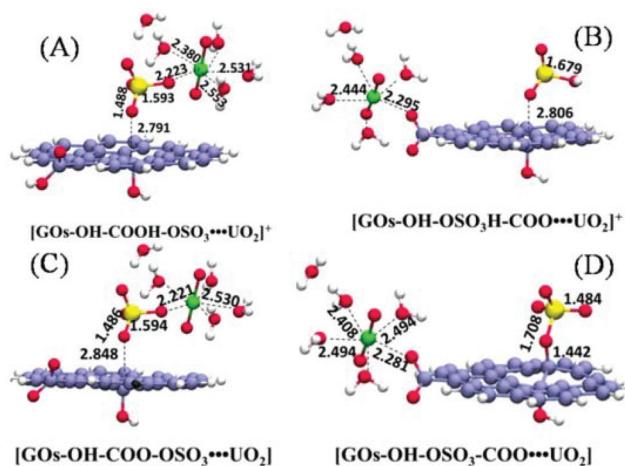
Fig. 10 Optimized models of GO complexes with uranyl species at pH = 2.0 (A and B) and at pH = 6.0 (C and D); bond lengths are in Å. Reproduced with permission from ref. 178. Copyright 2017 Elsevier.

indicating the greater stability of the uranyl-sulfonyl at ultra-low pH.[178] Fig. 10 shows DFT-optimized geometries of carboxyl and sulfonyl groups with uranyl complexes at pH = 2.0 (Fig. 10A and B) and pH = 6.0 (Fig. 10C and D).

Similar DFT calculations for the determination of adsorption states can be found in our previously published work.[24,64,87,179] The binding energies of Eu(III) on CNTs were found to be much higher than those of 243Am(III) on CNTs on the basis of DTF calculations, indicating that Eu(III) could form stronger complexes with the oxygen-containing functional groups of CNTs than 243Am(III), consistent with the experimental results of the higher sorption capacity of CNTs for Eu(III).[24] However, for the polymer-based composites as adsorbents, almost no theoretical calculations have been carried out to simulate the adsorption states, which is important to further understand the mechanism and the experimental results.

5. Post-treatment of adsorption process

5.1. Separation of the adsorbents

It is unavoidable to separate the adsorbents from the adsorption suspension either in experimental investigation or in the real applications. Generally, centrifugation and filtration are conventionally applied in the separation. For nanoparticles, the requirements for centrifugation or filtration are relatively greater than for larger particles with higher centrifugal force and finer filter holes. For polymer-based composites, the polymeric framework extending into the micrometer-scale would favor the centrifugation and filtration process, even when the composites were comprised of the nanoparticle counterparts. Ideally, if the loaded adsorbents could be separated from the solution by simple settlement, the power consumption can be reduced in the post-treatment process. Particularly, in the

mentioned various composites, magnetic polymer composites show great advantages due to the efficient and no power-consumption magnetic separation. In addition, the magnetic separations can be carried out without too much attention to the surface charge of loaded adsorbents, pH and ionic concentration of the adsorption solutions.[180]

5.2. Regeneration and reuse of polymer-based nano-adsorbents

Regeneration of the used adsorbent is of great importance for the possible practical application of the adsorbent materials in water remediation. An ideal regeneration process should be able to recover the initial adsorption behavior of the adsorbents although in the quantities of the present studies on metal ion removal *via* adsorption onto adsorbents, desorption and regeneration of the adsorbents are of less concern. For efficient desorption, the selection of a suitable eluent is often determined by the adsorption mechanism, the adsorbate and the adsorbent. Usually, the most commonly used desorption solutions are basic solutions and acid solutions to elute the metal ions from the loaded adsorbents. In contrast to that used in the adsorption process, the desorption of heavy metal cations is mainly conducted in acid solutions like dilute HNO_3 and HCl. For example, in work by Liu *et al.*, desorption studies were carried out by dispersing used magnetic chitosan nanocomposites in weak acetum solution and sonicating the mixture suspension.[145] The resulting concentration of Pb(II) in the eluent was about 32.32 mg L^{-1}. After treating with deionized water to neutralize, the adsorbent was explored for succeeding Pb(II) removal cycles. This procedure was repeated for up to six cycles. Although the removal efficiency was gradually reduced in the later cycles, it was still above 93% in the last cycle. The desorption of metallic oxyanions such as arsenic and chromium is conducted in basic solutions like NaOH solution in most studies. The reusability of chitosan zerovalent iron nanoparticle (CIN) towards arsenic removal was presented, where desorption was conducted with 0.1 M NaOH solution. About 50–60% of adsorbed As(V)/As(III) can be desorbed during the desorption cycles and no decrease in uptake capacity was found after five cycles.[181] Similar adsorbent regeneration and reuse was studied by Juan *et al.* for As(V) removal on functionalized magnetic materials.[182] However, it should be mentioned that the regeneration and reuse of polymer-based adsorbents should be of greater concern in future investigations, including the novel eluent method and other conditions of exploration.[183]

6. Conclusions and future perspectives

In conclusion, we have reviewed the recent works on the preparation of polymer composites and their application in the efficient removal of heavy metal ions from aqueous solutions under different conditions. A survey of related literature reveals that versatile polymer-based composites have been

applied for the removal of metal ions from wastewater solutions with the combination of polymers, carbon materials, clay minerals, magnetic nanoparticles and metal nanoparticles. Such counterparts themselves are also widely used for wastewater remediation, and after being incorporated within the polymer matrix, the adsorption capacity, mechanical strength, recycling performance, separation from solution are significantly improved. The involved polymers are not only present as supports for the other counterparts but also function as stabilizers, rigid frames and chelating materials. The various incorporated counterparts also provide effective chelating sites, magnetism and reducibility, *etc.* The methods for the preparation of the composites have been classified and discussed individually. The analysis and features of the adsorption process have been summarized comprehensively and discussed in detail, including batch experiments and the macro/microanalysis. The adsorption capacities of such polymer-based composites have been compared with other conventional materials. It was revealed that the polymer-based composites offer strong chelating capabilities towards heavy metal ions, fast adsorption kinetics and good regeneration ability with the synergistic effect of the polymers and various counterparts. Nevertheless, the mentioned materials and the preparation methods have not been scaled up from the laboratory to industrial applications and there is little research on estimating the production cost and the possibility for practical utilization. In addition, there still exist several issues that need to be clarified in the near future.

1. There should be some uniform criteria to evaluate the adsorption capacity of each specific heavy metal, such as temperature, pH, adsorbent/metal ion concentration, *etc.*, for clear comparisons between different kinds of adsorbents.

2. The desorption process should be investigated in detail and more reliable methods for adsorbent regeneration need to be developed.

3. More durable polymer-based composites with better regeneration ability should be explored and the long-term performance of adsorbents should be evaluated for permanent usage, not only for a few reuse cycles. The long-term performance is crucial for the real applications.

4. The toxicity of the polymer and the counterparts in the composites and the 'green chemistry' concept should be considered in the material design to avoid secondary pollution.

5. The mechanism of the adsorption process needs to be clarified using more advanced analytical techniques and characterization methods such as XAS, EXAFS, theoretical simulation and even the *in situ* techniques to gain insight at the molecular level about the removal process and the interaction mechanism.

6. More efforts should be devoted to the selective adsorption of heavy metal ions on polymer-based composites in the presence of multi-metal ions, besides that of the well-studied single-metal adsorption. The high selectivity of the polymer-based composites is important for the elimination of the low concentration of target metal ions from complicated systems.

7. More advanced polymer-based composites with high stability, and environmental friendliness should be developed with considerations given to low price and the possibility for large-scale preparation. For real applications, the price is an important parameter for the large-scale application.

8. There should be efficient separation of polymer-based composites from aqueous solutions after their application in the adsorption of metal ions. The polymer-based composites may become the pollutants if they remain in solution.

Conflicts of interest

There are no conflicts to declare.

Acknowledgements

Notes and references

1 T. Yao, T. Cui, J. Wu, Q. Chen, S. Lu and K. Sun, *Polym. Chem.*, 2011, **2**, 2893–2899.

2 M. R. Awual, S. Urata, A. Jyo, M. Tamada and A. Katakai, *Water Res.*, 2008, **42**, 689–696.

3 J. E. Efome, D. Rana, T. Matsuura and C. Q. Lan, *J. Mater. Chem. A*, 2018, **6**, 4550–4555.

4 C. Chen and X. Wang, *Ind. Eng. Chem. Res.*, 2006, **45**, 9144–9149.

5 G. Zhao, J. Li, X. Ren, C. Chen and X. Wang, *Environ. Sci. Technol.*, 2011, **45**, 10454–10462.

6 G. Sheng, J. Li, D. Shao, J. Hu, C. Chen, Y. Chen and X. Wang, *J. Hazard. Mater.*, 2010, **178**, 333–340.

7 S. Zhang, M. Zeng, W. Xu, J. Li, J. Li, J. Xu and X. Wang, *Dalton Trans.*, 2013, **42**, 7854–7858.

8 C. Ding, W. Cheng, X. Wang, Z.-Y. Wu, Y. Sun, C. Chen, X. Wang and S.-H. Yu, *J. Hazard. Mater.*, 2016, **313**, 253–261.

9 M. Liu, T. Wen, X. Wu, C. Chen, J. Hu, J. Li and X. Wang, *Dalton Trans.*, 2013, **42**, 14710–14717.

10 G. Zhao, X. Ren, X. Gao, X. Tan, J. Li, C. Chen, Y. Huang and X. Wang, *Dalton Trans.*, 2011, **40**, 10945–10952.

11 X. Ren, J. Li, X. Tan and X. Wang, *Dalton Trans.*, 2013, **42**, 5266–5274.

12 G. Zhao, H. Zhang, Q. Fan, X. Ren, J. Li, Y. Chen and X. Wang, *J. Hazard. Mater.*, 2010, **173**, 661–668.

13 X. Wang, C. Chen, J. Du, X. Tan, D. Xu and S. Yu, *Environ. Sci. Technol.*, 2005, **39**, 7084–7088.

14 X. Tan, M. Fang, X. Ren, H. Mei, D. Shao and X. Wang, *Environ. Sci. Technol.*, 2014, **48**, 13138–13145.

15 X. Tan, Q. Fan, X. Wang and B. Grambow, *Environ. Sci. Technol.*, 2009, **43**, 3115–3121.

16 X. Tan, M. Fang, J. Li, Y. Lu and X. Wang, *J. Hazard. Mater.*, 2009, **168**, 458–465.

17 C. Chen and X. Wang, *Appl. Radiat. Isot.*, 2007, **65**, 155–163.

18 Y. Huang, J. Li, X. Chen and X. Wang, *RSC Adv.*, 2014, **4**, 62160–62178.

19 R. Hu, D. Shao and X. Wang, *Polym. Chem.*, 2014, **5**, 6207–6215.

20 D. Shao, Z. Jiang, X. Wang, J. Li and Y. Meng, *J. Phys. Chem. B*, 2009, **113**, 860–864.

21 Y. Zou, X. Wang, A. Khan, P. Wang, Y. Liu, A. Alsaedi, T. Hayat and X. Wang, *Environ. Sci. Technol.*, 2016, **50**, 7290–7304.

22 S. Yu, X. Wang, H. Pang, R. Zhang, W. Song, D. Fu, T. Hayat and X. Wang, *Chem. Eng. J.*, 2018, **333**, 343–360.

23 J. Li, X. Wang, G. Zhao, C. Chen, Z. Chai, A. Alsaedi, T. Hayat and X. Wang, *Chem. Soc. Rev.*, 2018, **47**, 2322–2356.

24 P. K. Mishra, R. Kumar and P. K. Rai, *Nanoscale*, 2018, **10**, 7257–7269.

25 R. Das, C. D. Vecitis, A. Schulze, B. Cao, A. F. Ismail, X. Lu, J. Chen and S. Ramakrishna, *Chem. Soc. Rev.*, 2017, **46**, 6946–7020.

26 A. Deliyanni Eleni, Z. Kyzas George, S. Triantafyllidis Kostas and A. Matis Kostas, *Open Chem.*, 2015, **13**, 699–708.

27 M. Hua, S. Zhang, B. Pan, W. Zhang, L. Lv and Q. Zhang, *J. Hazard. Mater.*, 2012, **211–212**, 317–331.

28 S. Li, X. Lu, Y. Xue, J. Lei, T. Zheng and C. Wang, *PLoS One*, 2012, **7**, e43328.

29 S. Zhang, M. Zeng, W. Xu, J. Li, J. Li, J. Xu and X. Wang, *Dalton Trans.*, 2013, **42**, 7854–7858.

30 B. Pan, B. Pan, W. Zhang, L. Lv, Q. Zhang and S. Zheng, *Chem. Eng. J.*, 2009, **151**, 19–29.

31 X. Zhao, L. Lv, B. Pan, W. Zhang, S. Zhang and Q. Zhang, *Chem. Eng. J.*, 2011, **170**, 381–394.

32 H. N. M. E. Mahmud, A. O. Huq and R. Binti Yahya, *RSC Adv.*, 2016, **6**, 14778–14791.

33 P. Cornel and H. Sontheimer, *Chem. Eng. Sci.*, 1986, **41**, 1791–1800.

34 D. Wang, X. Wang, Y. Zhao, H. Gao, Y. Xing and H. Yang, *Polym. Chem.*, 2012, **3**, 914–919.

35 B. L. Rivas, J. Sánchez and B. F. Urbano, *Polym. Int.*, 2016, **65**, 255–267.

36 T. López-León, E. Carvalho, B. Seijo, J. Ortega-Vinuesa and D. Bastos-González, *J. Colloid Interface Sci.*, 2005, **283**, 344–351.

37 A. Wu, J. Jia and S. Luan, *Colloids Surf., A*, 2011, **384**, 180–185.

38 S. Venkateswarlu and M. Yoon, *ACS Appl. Mater. Interfaces*, 2015, **7**, 25362–25372.

39 D. Shao, J. Hu, C. Chen, G. Sheng, X. Ren and X. Wang, *J. Phys. Chem. C*, 2010, **114**, 21524–21530.

40 Q. Zhang, B. Pan, X. Chen, W. Zhang, B. Pan, Q. Zhang, L. Lv and X. Zhao, *Sci. China, Ser. B: Chem.*, 2008, **51**, 379–385.

41 L. Cumbal and A. K. SenGupta, *Environ. Sci. Technol.*, 2005, **39**, 6508–6515.

42 B. Samiey, C.-H. Cheng and J. Wu, *Materials*, 2014, **7**, 673–726.

43 M. Bhaumik, H. J. Choi, R. I. McCrindle and A. Maity, *J. Colloid Interface Sci.*, 2014, **425**, 75–82.

44 G.-B. Cai, G.-X. Zhao, X.-K. Wang and S.-H. Yu, *J. Phys. Chem. C*, 2010, **114**, 12948–12954.

45 S. Ghorai, A. Sarkar, M. Raoufi, A. B. Panda, H. Schönherr and S. Pal, *ACS Appl. Mater. Interfaces*, 2014, **6**, 4766–4777.

46 Q. Zhang, B. Pan, S. Zhang, J. Wang, W. Zhang and L. Lv, *J. Nanopart. Res.*, 2011, **13**, 5355.

47 T. Anirudhan and M. Ramachandran, *Ind. Eng. Chem. Res.*, 2008, **47**, 6175–6184.

48 L. Wang, X.-L. Wu, W.-H. Xu, X.-J. Huang, J.-H. Liu and A.-W. Xu, *ACS Appl. Mater. Interfaces*, 2012, **4**, 2686–2692.

49 Y. Wang, X. Teng, J.-S. Wang and H. Yang, *Nano Lett.*, 2003, **3**, 789–793.

50 C.-L. Huang and E. Matijevic, *J. Mater. Res.*, 1995, **10**, 1327–1336.

51 T. A. Saleh, A. Sarı and M. Tuzen, *Chem. Eng. J.*, 2017, **307**, 230–238.

52 Y. Liu, A. Wang and R. Claus, *J. Phys. Chem. B*, 1997, **101**, 1385–1388.

53 G. Sharma, D. Pathania, M. Naushad and N. Kothiyal, *Chem. Eng. J.*, 2014, **251**, 413–421.

54 Q. Yu, P. Wu, P. Xu, L. Li, T. Liu and L. Zhao, *Green Chem.*, 2008, **10**, 1061–1067.

55 M. Naushad, T. Ahamad, G. Sharma, H. Ala'a, A. B. Albadarin, M. M. Alam, Z. A. ALOthman, S. M. Alshehri and A. A. Ghfar, *Chem. Eng. J.*, 2016, **300**, 306–316.

56 E. Vunain, A. Mishra and R. Krause, *J. Inorg. Organomet. Polym. Mater.*, 2013, **23**, 293–305.

57 A. Kumar, G. Sharma, M. Naushad and S. Thakur, *Chem. Eng. J.*, 2015, **280**, 175–187.

58 G. Kickelbick, *Prog. Polym. Sci.*, 2003, **28**, 83–114.

59 H. L. Frisch, Y. p. Xue, S. Maaref, G. Beaucage, Z. Pu and J. E. Mark, *Pseudo interpenetrating polymer networks and interpenetrating polymer networks of zeolite 13 X and polystyrene and poly (ethyl acrylate)*, 1996.

60 X.-F. Wen, K. Wang, P.-H. Pi, J.-X. Yang, Z.-Q. Cai, L.-j. Zhang, Y. Qian, Z.-R. Yang, D.-f. Zheng and J. Cheng, *Appl. Surf. Sci.*, 2011, **258**, 991–998.

61 T. Ogoshi and Y. Chujo, *Compos. Interfaces*, 2005, **11**, 539–566.

62 P. Hajji, L. David, J. Gerard, H. Kaddami, J. Pascault and G. Vigier, *MRS Online Proc. Libr.*, 1999, **576**, 357.

63 C. Avadhani and Y. Chujo, *Appl. Organomet. Chem.*, 1997, **11**, 153–161.

64 M.-T. Wu, Y.-L. Tsai, C.-W. Chiu and C.-C. Cheng, *RSC Adv.*, 2016, **6**, 104754–104762.

65 H. Javadian, *J. Ind. Eng. Chem.*, 2014, **20**, 4233–4241.

66 H. Javadian, F. Z. Sorkhrodi and B. B. Koutenaei, *J. Ind. Eng. Chem.*, 2014, **20**, 3678–3688.

67 J. Wang, K. Pan, Q. He and B. Cao, *J. Hazard. Mater.*, 2013, **244**, 121–129.

68 M. Bhaumik, A. Maity, V. Srinivasu and M. S. Onyango, *Chem. Eng. J.*, 2012, **181**, 323–333.

69 F. Checkol, A. Elfwing, G. Greczynski, S. Mehretie, O. Inganäs and S. Admassie, *Adv. Sustainable Syst.*, 2018, **2**, 1700114.

70 H. Yan, L. Yang, Z. Yang, H. Yang, A. Li and R. Cheng, *J. Hazard. Mater.*, 2012, **229**, 371–380.

71 L.-L. Hwang, J.-C. Chen and M.-Y. Wey, *Desalination*, 2013, **313**, 166–175.

72 S. Chowdhury and R. Balasubramanian, *Adv. Colloid Interface Sci.*, 2014, **204**, 35–56.

73 D. Shao, J. Hu and X. Wang, *Plasma Processes Polym.*, 2010, **7**, 977–985.

74 W. N. Nyairo, Y. R. Eker, C. Kowenje, I. Akin, H. Bingol, A. Tor and D. M. Ongeri, *Sep. Sci. Technol.*, 2018, 1–13.

75 Y. Chen, L. Chen, H. Bai and L. Li, *J. Mater. Chem. A*, 2013, **1**, 1992–2001.

76 Y. Q. He, N. N. Zhang and X. D. Wang, *Chin. Chem. Lett.*, 2011, **22**, 859–862.

77 L. Fan, C. Luo, M. Sun, X. Li and H. Qiu, *Colloids Surf., B*, 2013, **103**, 523–529.

78 L. Li, L. Fan, M. Sun, H. Qiu, X. Li, H. Duan and C. Luo, *Colloids Surf., B*, 2013, **107**, 76–83.

79 Y. Cai, C. Wu, Z. Liu, L. Zhang, L. Chen, J. Wang, X. Wang, S. Yang and S. Wang, *Environ. Sci.: Nano*, 2017, **4**, 1876–1886.

80 Y. L. F. Musico, C. M. Santos, M. L. P. Dalida and D. F. Rodrigues, *J. Mater. Chem. A*, 2013, **1**, 3789–3796.

81 V. Chandra and K. S. Kim, *Chem. Commun.*, 2011, **47**, 3942–3944.

82 D. Wang, L. Liu, X. Jiang, J. Yu and X. Chen, *Colloids Surf., A*, 2015, **466**, 166–173.

83 R. Li, L. Liu and F. Yang, *Chem. Eng. J.*, 2013, **229**, 460–468.

84 Y. Yang, Y. Xie, L. Pang, M. Li, X. Song, J. Wen and H. Zhao, *Langmuir*, 2013, **29**, 10727–10736.

85 W. Song, X. Wang, Q. Wang, D. Shao and X. Wang, *Phys. Chem. Chem. Phys.*, 2015, **17**, 398–406.

86 Y. Zhao, X. Wang, J. Li and X. Wang, *Polym. Chem.*, 2015, **6**, 5376–5384.

87 Y. Yu, Z. Hu, Z. Chen, J. Yang, H. Gao and Z. Chen, *RSC Adv.*, 2016, **6**, 97523–97531.

88 M. Ghoul, M. Bacquet and M. Morcellet, *Water Res.*, 2003, **37**, 729–734.

89 P. Yin, Q. Xu, R. Qu, G. Zhao and Y. Sun, *J. Hazard. Mater.*, 2010, **173**, 710–716.

90 B. Gao, Y. Gao and Y. Li, *Chem. Eng. J.*, 2010, **158**, 542–549.

91 Y. Liu, Z. Liu, J. Gao, J. Dai, J. Han, Y. Wang, J. Xie and Y. Yan, *J. Hazard. Mater.*, 2011, **186**, 197–205.

92 S. Wu, F. Li, H. Wang, L. Fu, B. Zhang and G. Li, *Polymer*, 2010, **51**, 6203–6211.

93 Q. Huang, M. Liu, J. Zhao, J. Chen, G. Zeng, H. Huang, J. Tian, Y. Wen, X. Zhang and Y. Wei, *Appl. Surf. Sci.*, 2018, **427**, 535–544.

94 G. Wei, K. Dong, Q. Liu, T. Gao and J. Yao, *J. Appl. Polym. Sci.*, 2018, **135**, 45839.

95 Q. Zhang, B. Pan, W. Zhang, B. Pan, L. Lv, X. Wang, J. Wu and X. Tao, *J. Hazard. Mater.*, 2009, **170**, 824–828.

96 R. Vivani, G. Alberti, F. Costantino and M. Nocchetti, *Microporous Mesoporous Mater.*, 2008, **107**, 58–70.

97 T. M. Suzuki, S. Kobayashi, D. A. P. Tanaka, M. A. L. Tanco, T. Nagase and Y. Onodera, *React. Funct. Polym.*, 2004, **58**, 131–138.

98 B. Pan, B. Pan, X. Chen, W. Zhang, X. Zhang, Q. Zhang, Q. Zhang and J. Chen, *Water Res.*, 2006, **40**, 2938–2946.

99 Q. Zhang, B. Pan, W. Zhang, B. Pan, L. Lv, X. Wang, J. Wu and X. Tao, *J. Hazard. Mater.*, 2009, **170**, 824–828.

100 R. Bushra, M. Shahadat, A. Ahmad, S. Nabi, K. Umar, M. Oves, A. Raeissi and M. Muneer, *J. Hazard. Mater.*, 2014, **264**, 481–489.

101 A. S. K. Kumar, S. Kalidhasan, V. Rajesh and N. Rajesh, *Ind. Eng. Chem. Res.*, 2011, **51**, 58–69.

102 U. Ulusoy and S. Şimşek, *J. Hazard. Mater.*, 2005, **127**, 163–171.

103 M. Khalek, G. A. Mahmoud and N. A. El-Kelesh, *Chem. Mater. Res.*, 2012, **2**, 1–12.

104 K. Z. Setshedi, M. Bhaumik, S. Songwane, M. S. Onyango and A. Maity, *Chem. Eng. J.*, 2013, **222**, 186–197.

105 D. Fan, X. Zhu, M. Xu and J. Yan, *J. Biol. Sci.*, 2006, **6**, 941–945.

106 N. Bleiman and Y. G. Mishael, *J. Hazard. Mater.*, 2010, **183**, 590–595.

107 I. Larraza, M. López-Gónzalez, T. Corrales and G. Marcelo, *J. Colloid Interface Sci.*, 2012, **385**, 24–33.

108 S. Pandey and S. B. Mishra, *J. Colloid Interface Sci.*, 2011, **361**, 509–520.

109 S. Hasan, T. K. Ghosh, D. S. Viswanath and V. M. Boddu, *J. Hazard. Mater.*, 2008, **152**, 826–837.

110 S. Hasan, A. Krishnaiah, T. K. Ghosh, D. S. Viswanath, V. M. Boddu and E. D. Smith, *Ind. Eng. Chem. Res.*, 2006, **45**, 5066–5077.

111 S. Kalyani, J. A. Priya, P. S. Rao and A. Krishnaiah, *Sep. Sci. Technol.*, 2005, **40**, 1483–1495.

112 Z. Fallah, H. Nasr Isfahani, M. Tajbakhsh, H. Tashakkorian and A. Amouei, *Cellulose*, 2018, **25**, 639–660.

113 T. Wen, Q. Fan, X. Tan, Y. Chen, C. Chen, A. Xu and X. Wang, *Polym. Chem.*, 2016, **7**, 785–794.

114 J. Li, C. Chen, R. Zhang and X. Wang, *Chem. – Asian J.*, 2015, **10**, 1410–1417.

115 X. Li, L. Ai and J. Jiang, *Chem. Eng. J.*, 2016, **288**, 789–797.

116 J. WooáLee and S. BináKim, *Nanoscale*, 2011, **3**, 3583–3585.

117 J. Li, C. Chen, K. Zhu and X. Wang, *J. Taiwan Inst. Chem. Eng.*, 2016, **59**, 389–394.

118 Z.-J. Li, L. Wang, L.-Y. Yuan, C.-L. Xiao, L. Mei, L.-R. Zheng, J. Zhang, J.-H. Yang, Y.-L. Zhao and Z.-T. Zhu, *J. Hazard. Mater.*, 2015, **290**, 26–33.

119 C. Wang, H. Luo, Z. Zhang, Y. Wu, J. Zhang and S. Chen, *J. Hazard. Mater.*, 2014, **268**, 124–131.

120 S. R. Kanel, B. Manning, L. Charlet and H. Choi, *Environ. Sci. Technol.*, 2005, **39**, 1291–1298.

121 H. Zhu, Y. Jia, X. Wu and H. Wang, *J. Hazard. Mater.*, 2009, **172**, 1591–1596.

122 H. Kim, H.-J. Hong, J. Jung, S.-H. Kim and J.-W. Yang, *J. Hazard. Mater.*, 2010, **176**, 1038–1043.

123 Q. Wang, H. Qian, Y. Yang, Z. Zhang, C. Naman and X. Xu, *J. Contam. Hydrol.*, 2010, **114**, 35–42.

124 X. Zhao, X. Dou, D. Mohan, C. U. Pittman Jr., Y. S. Ok and X. Jin, *Chem. Eng. J.*, 2014, **247**, 250–257.

125 M. Kim, K. Sohn, H. B. Na and T. Hyeon, *Nano Lett.*, 2002, **2**, 1383–1387.

126 S. M. Ponder, J. G. Darab and T. E. Mallouk, *Environ. Sci. Technol.*, 2000, **34**, 2564–2569.

127 J. Li, H. Li, Y. Zhu, Y. Hao, X. Sun and L. Wang, *Appl. Surf. Sci.*, 2011, **258**, 657–661.

128 K. V. G. Ravikumar, S. Argulwar, S. V. Sudakaran, M. Pulimi, N. Chandrasekaran and A. Mukherjee, *Environ. Technol. Innovat.*, 2018, **9**, 122–133.

129 S.-J. Wu, T.-H. Liou and F.-L. Mi, *Bioresour. Technol.*, 2009, **100**, 4348–4353.

130 D. H. K. Reddy and S.-M. Lee, *Adv. Colloid Interface Sci.*, 2013, **201**, 68–93.

131 F.-C. Wu, R.-L. Tseng and R.-S. Juang, *J. Environ. Manage.*, 2010, **91**, 798–806.

132 A. Z. M. Badruddoza, Z. B. Z. Shawon, W. J. D. Tay, K. Hidajat and M. S. Uddin, *Carbohydr. Polym.*, 2013, **91**, 322–332.

133 M. Chen, W. Jiang, F. Wang, P. Shen, P. Ma, J. Gu, J. Mao and F. Li, *Appl. Surf. Sci.*, 2013, **286**, 249–256.

134 M. Bhaumik, T. Y. Leswifi, A. Maity, V. Srinivasu and M. S. Onyango, *J. Hazard. Mater.*, 2011, **186**, 150–159.

135 M. Bhaumik, A. Maity, V. Srinivasu and M. S. Onyango, *J. Hazard. Mater.*, 2011, **190**, 381–390.

136 M. Takafuji, S. Ide, H. Ihara and Z. Xu, *Chem. Mater.*, 2004, **16**, 1977–1983.

137 H. Wang, X. Yuan, Y. Wu, X. Chen, L. Leng, H. Wang, H. Li and G. Zeng, *Chem. Eng. J.*, 2015, **262**, 597–606.

138 C. I. Covaliu, D. Berger, C. Matei, L. Diamandescu, E. Vasile, C. Cristea, V. Ionita and H. Iovu, *J. Nanopart. Res.*, 2011, **13**, 6169–6180.

139 F.-Y. Cheng, C.-H. Su, Y.-S. Yang, C.-S. Yeh, C.-Y. Tsai, C.-L. Wu, M.-T. Wu and D.-B. Shieh, *Biomaterials*, 2005, **26**, 729–738.

140 J. Singh, M. Srivastava, J. Dutta and P. Dutta, *Int. J. Biol. Macromol.*, 2011, **48**, 170–176.

141 R. Qin, F. Li, M. Chen and W. Jiang, *Appl. Surf. Sci.*, 2009, **256**, 27–32.

142 J. Singh, M. Srivastava, P. Kalita and B. D. Malhotra, *Process Biochem.*, 2012, **47**, 2189–2198.

143 L. Luo, Q. Li, Y. Xu, Y. Ding, X. Wang, D. Deng and Y. Xu, *Sens. Actuators, B*, 2010, **145**, 293–298.

144 Y. Lin, W. Yao, Y. Cheng, H. Qian, X. Wang, Y. Ding, W. Wu and X. Jiang, *J. Mater. Chem.*, 2012, **22**, 5684–5693.

145 X. Liu, Q. Hu, Z. Fang, X. Zhang and B. Zhang, *Langmuir*, 2008, **25**, 3–8.

146 L. Zhou, Y. Wang, Z. Liu and Q. Huang, *J. Hazard. Mater.*, 2009, **161**, 995–1002.

147 S. Yang, P. Zong, J. Hu, G. Sheng, Q. Wang and X. Wang, *Chem. Eng. J.*, 2013, **214**, 376–385.

148 J. Li, C. Chen, Y. Zhao, J. Hu, D. Shao and X. Wang, *Chem. Eng. J.*, 2013, **229**, 296–303.

149 D. Shao, X. Wang, J. Li, Y. Huang, X. Ren, G. Hou and X. Wang, *Environ. Sci.: Water Res. Technol.*, 2015, **1**, 169–176.

150 M. Monier and D. Abdel-Latif, *J. Hazard. Mater.*, 2012, **209**, 240–249.

151 Y. Ho, G. McKay, D. Wase and C. Forster, *Adsorpt. Sci. Technol.*, 2000, **18**, 639–650.

152 Y. Chen and J. Wang, *Nucl. Eng. Des.*, 2012, **242**, 445–451.

153 C. Yuwei and W. Jianlong, *Chem. Eng. J.*, 2011, **168**, 286–292.

154 Z. Yu, X. Zhang and Y. Huang, *Ind. Eng. Chem. Res.*, 2013, **52**, 11956–11966.

155 Y. Sun, S. Lu, X. Wang, C. Xu, J. Li, C. Chen, J. Chen, T. Hayat, A. Alsaedi, N. S. Alharbi and X. Wang, *Environ. Sci. Technol.*, 2017, **51**, 12274–12282.

156 G. Sheng, S. Yang, J. Sheng, J. Hu, X. Tan and X. Wang, *Environ. Sci. Technol.*, 2011, **45**, 7718–7726.

157 Y. Zou, X. Wang, Y. Ai, Y. Liu, J. Li, Y. Ji and X. Wang, *Environ. Sci. Technol.*, 2016, **50**, 3658–3667.

158 X. Wang, S. Yang, W. Shi, J. Li, T. Hayat and X. Wang, *Environ. Sci. Technol.*, 2015, **49**, 11721–11728.

159 D. Zhao, L. Chen, M. Xu, S. Feng, Y. Ding, M. Wakeel, N. S. Alharbi and C. Chen, *ACS Sustainable Chem. Eng.*, 2017, **5**, 10290–10297.

160 Y. Sun, S. Yang, Y. Chen, C. Ding, W. Cheng and X. Wang, *Environ. Sci. Technol.*, 2015, **49**, 4255–4262.

161 X. Wang, Q. Fan, S. Yu, Z. Chen, Y. Ai, Y. Sun, A. Hobiny, A. Alsaedi and X. Wang, *Chem. Eng. J.*, 2016, **287**, 448–455.

162 G. D. Vuković, A. D. Marinković, S. D. Škapin, M. Đ. Ristić, R. Aleksić, A. A. Perić-Grujić and P. S. Uskoković, *Chem. Eng. J.*, 2011, **173**, 855–865.

163 E. Deliyanni, A. Arabatzidou, N. Tzoupanos and K. A. Matis, *Adsorpt. Sci. Technol.*, 2012, **30**, 627–645.

164 M. Karnib, A. Kabbani, H. Holail and Z. Olama, *Energy Procedia*, 2014, **50**, 113–120.

165 E. Deliyanni, T. J. Bandosz and K. A. Matis, *J. Chem. Technol. Biotechnol.*, 2013, **88**, 1058–1066.

166 Y.-H. Chen and F.-A. Li, *J. Colloid Interface Sci.*, 2010, **347**, 277–281.

167 K. E. Engates and H. J. Shipley, *Environ. Sci. Pollut. Res.*, 2011, **18**, 386–395.

168 E. Eren, *J. Hazard. Mater.*, 2009, **165**, 63–70.

169 E. Eren, A. Tabak and B. Eren, *Desalination*, 2010, **257**, 163–169.

170 K. Anoop Krishnan and T. S. Anirudhan, *J. Hazard. Mater.*, 2002, **92**, 161–183.

171 S. Q. Memon, N. Memon, S. W. Shah, M. Y. Khuhawar and M. I. Bhanger, *J. Hazard. Mater.*, 2007, **139**, 116–121.

172 S. Nethaji, A. Sivasamy and A. B. Mandal, *Bioresour. Technol.*, 2013, **134**, 94–100.

173 Y. Sun, Z.-Y. Wu, X. Wang, C. Ding, W. Cheng, S.-H. Yu and X. Wang, *Environ. Sci. Technol.*, 2016, **50**, 4459–4467.

174 Y. Sun, C. Ding, W. Cheng and X. Wang, *J. Hazard. Mater.*, 2014, **280**, 399–408.

175 Y. Sun, X. Wang, W. Song, S. Lu, C. Chen and X. Wang, *Environ. Sci.: Nano*, 2017, **4**, 222–232.

176 Y. Sun, Q. Wang, C. Chen, X. Tan and X. Wang, *Environ. Sci. Technol.*, 2012, **46**, 6020–6027.

177 W. Cheng, C. Ding, Q. Wu, X. Wang, Y. Sun, W. Shi, T. Hayat, A. Alsaedi, Z. Chai and X. Wang, *Environ. Sci.: Nano*, 2017, **4**, 1124–1131.

178 Y. Sun, X. Wang, Y. Ai, Z. Yu, W. Huang, C. Chen, T. Hayat, A. Alsaedi and X. Wang, *Chem. Eng. J.*, 2017, **310**, 292–299.

179 Y. Ai, Y. Liu, W. Y. Lan, J. R. Jin, J. L. Xing, Y. D. Zou, C. F. Zhao and X. K. Wang, *Chem. Eng. J.*, 2018, **343**, 460–466.

180 C. T. Yavuz, J. T. Mayo, W. W. Yu, A. Prakash, J. C. Falkner, S. Yean, L. Cong, H. J. Shipley, A. Kan, M. Tomson, D. Natelson and V. L. Colvin, *Science*, 2006, **314**, 964–967.

181 A. Gupta, M. Yunus and N. Sankararamakrishnan, *Chemosphere*, 2012, **86**, 150–155.

182 S. Juan, B. Eugenio and O. Inmaculada, *J. Chem. Technol. Biotechnol.*, 2014, **89**, 909–918.

183 P. C. Gu, S. Zhang, X. Li, X. X. Wang, T. Wen, R. Jehan, A. Alsaedi, T. Hayat and X. K. Wang, *Environ. Pollut.*, 2018, **240**, 493–505.